# Unveiling Accretion in Massive Protostars through High-Resolution Studies of Jets and Outflows


Ciriaco Goddi

Università degli Studi di Cagliari

Universidade de São Paulo



USP Universidade de São Paulo

IAG INSTITUTO DE ASTRONOMIA, GEOFÍSICA E CIÊNCIAS ATMOSFÉRICAS

Università degli Studi di Cagliari

INAF Istituto Nazionale di Astrofisica

# VLBI observations of H2O masers in high-mass star forming regions

- Maser radiation originates from compact and bright maser spots
  => ideal targets of radio (very long baseline) interferometry (VLBI)
- They are excellent probes of local conditions and kinematics very close to the YSO (<100 AU)
  =>excitation at T ≥ 200-2000 K and n>107-10 cm-3
- Multi-epoch studies provide gas 3-D kinematics
  => proper motions + l.o.s velocities at the *highest angular resolution [O(mas)]*
- **Real gas kinematics, not illumination patterns!**
  **=> morphology of individual spots as well as overall structure of the maser source is preserved over time**

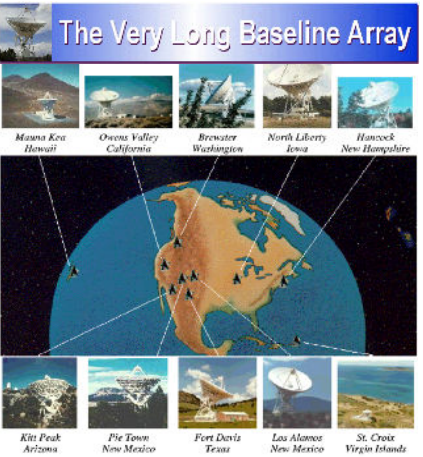



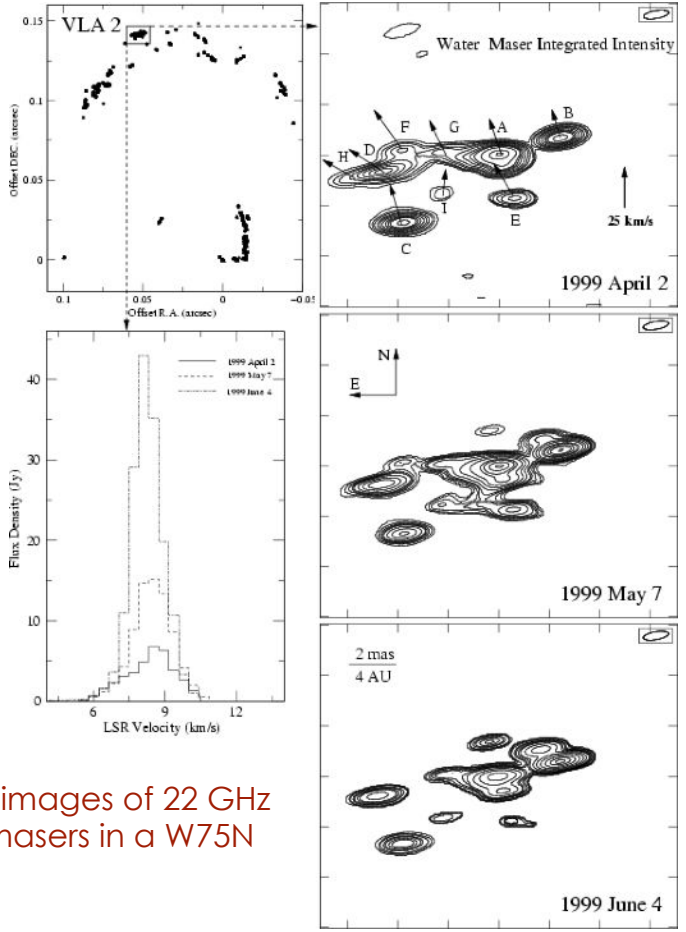


VLBA images of 22 GHz $H_2O$ masers in a W75N

*Goddi, Moscadelli,Torrelles, Uscanga, Cesaroni 2006*

# S255

Keplerian disk model

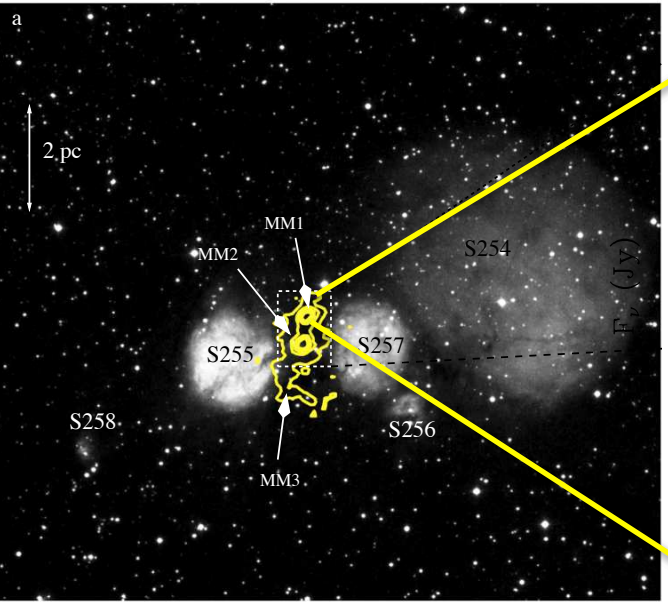


Water maser spectral profile with Medicina

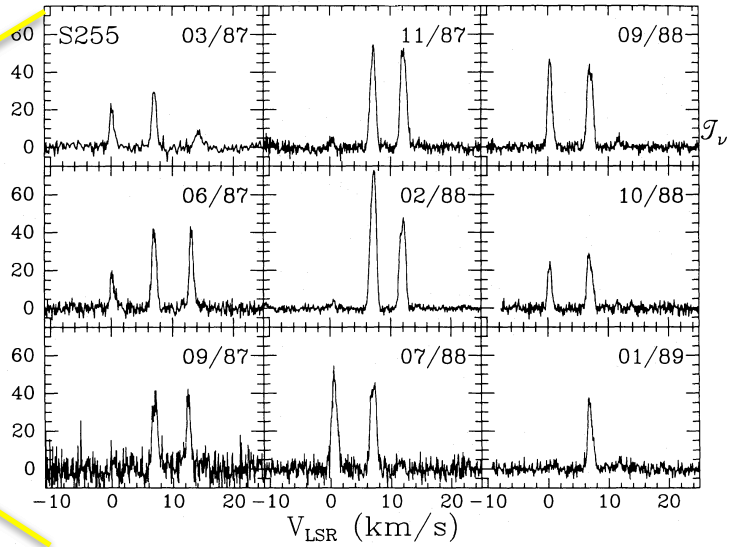


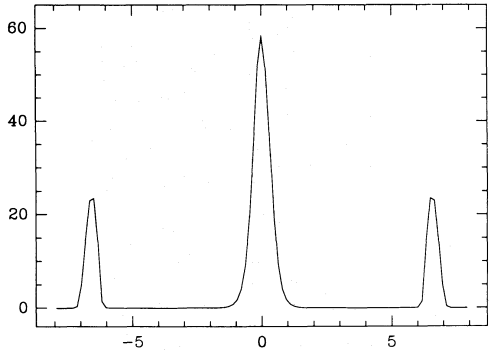


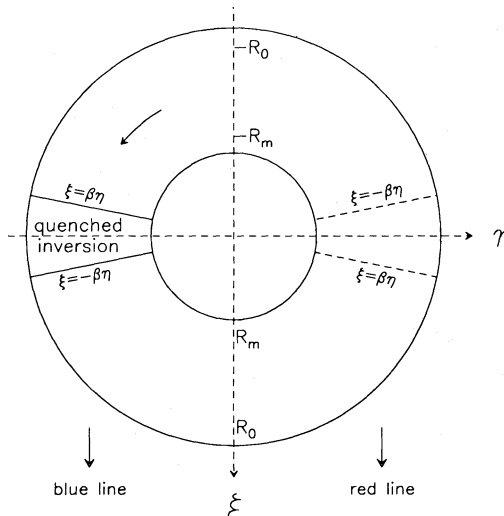


Minier, Peretto, Longmore, Burton, Cesaroni, Goddi, et al. 2006

Cesaroni 1990

objects have a triple line profile that is believed to be typical of accretion masering disks.

One of them (S 255) was monitored for about two years and we detected a remarkable anticorrelated variability of the two side lines. This is interpreted in terms of emission from a rotating Keplerian disk with population inversion confined in a given corona; the anticorrelated variability is the consequence of the radiative contact assured by the maser photons between the diametrically opposed sectors of this torus and occurs when population inversion is quenched in only one part of the disk.

The radiative transfer equation has been numerically solved for this particular scenario and the calculated spectra qualitatively agree with the observed ones. As an indirect result we find that the pumping for this maser has to be radiative: this conclusion is not contradicted by the infrared data available for the object. Finally the mass of the central (proto) star is estimated to be $\sim 18\, M_{\odot}$.

*Acknowledgements.* I gratefully acknowledge the Radioastronomy Group of the Arcetri Astrophysical Observatory and the operators of the VLBI station of Medicina for their precious collaboration during the observations and data reduction. I specially thank M. Felli for critically reading the manuscript.

## Appendix

### A. Radiative transfer in a Keplerian disk

The aim of this appendix is to solve numerically the radiative transfer equation in a Keplerian disk in two cases: 1) the population inversion is uniform within $R_m < R < R_0$ (Sect. A.1) and 2) the inversion is quenched in a small sector (Sect. A.2).

As a first remark we stress a very important point: our treatment aims to reproduce only the *qualitative* behaviour of the line profile, since the *quantitative* treatment of the line flux would require a specific pumping model that is well beyond our scope. Therefore we'll deliberately ignore any complication that would only change the spectrum intensity, but not its shape.

We suppose that the disk axis lies in the plane of the sky and that the line of sight is parallel to the $x$ axis with the observer at $x = +\infty$. The disk is rotating counterclockwise if observed from $z > 0$ (see also Fig. 6).

Following Alcock and Ross (1985a) the radiative transfer equation can be written in the form:

$$\frac{\mathrm{d}I_\nu}{\mathrm{d}x} = \frac{h\nu_{\mathrm{H_2O}}}{4\pi}\phi(v - v_0(x,y))[(n_2 - n_1)BI_\nu + n_2 A] \tag{8}$$

where $I_\nu$ is the brightness at frequency $\nu$, $\nu_{\mathrm{H_2O}} = 22.3$ GHz, $A$ and $B$ are the Einstein coefficients, $h$ is the Planck constant, $n_1$ and $n_2$ are the number density of the molecule in the lower and upper levels of the maser transition and $\phi$ is the normalized line profile function given – for Doppler broadening – by

$$\phi(v - v_0) = \frac{2}{\Delta v}\sqrt{\frac{\ln 2}{\pi}}\, \mathrm{e}^{-4\ln 2\left(\frac{v - v_0}{\Delta v}\right)^2}$$

with $\Delta v \equiv$ FWHM of the line. The frequency of the line is Doppler shifted according to the expression

$$v_0(\xi,\eta) \equiv \nu_{\mathrm{H_2O}}\left(1 - \frac{v_\xi(\xi,\eta)}{c}\right),$$

$$v_\xi \equiv \frac{\eta}{\mathscr{R}} v(\mathscr{R}), \quad \mathscr{R} \equiv \sqrt{\xi^2 + \eta^2},$$

$$\xi \equiv \frac{x}{L}, \quad \eta \equiv \frac{y}{L}, \quad \text{with} \quad L \equiv \frac{4\pi\Delta v}{nB h\nu_{\mathrm{H_2O}}}\,\frac{P_{12} + P_{21} + 2C}{P_{12} - P_{21}},$$

where $v_0$ is the Doppler shifted frequency of the line, $L$ is the unsaturated gain length, $n$ is the total number density in the maser levels, $C$ is the collisional rate between these levels and $P$'s describe all exchange processes with the other molecular levels.

Even if it is not strictly correct for $H_2O$, we have assumed statistical weights unity in order to simplify the problem. The $n_1$ and $n_2$ densities can be determined by

$$n_2(P_{21} + C + BJ + A) = n_1(P_{12} + C + BJ),$$

$$n_1 + n_2 = n,$$

where $J$ is the profile averaged mean intensity defined by

$$J \equiv \int_0^{+\infty} \phi J_\nu \mathrm{d}\nu$$

with

$$J_\nu \equiv \frac{1}{4\pi}\int_{4\pi} I_\nu \mathrm{d}\Omega.$$

Neglecting $A$ in comparison with $P_{12} - P_{21}$ one obtains

$$\frac{n_2 - n_1}{n} = \frac{P_{12} - P_{21}}{P_{12} + P_{21} + 2C + 2BJ}. \tag{9}$$

By means of Eq. (9) we can express (8) in the alternative form

$$\frac{\mathrm{d}\mathscr{T}_\nu}{\mathrm{d}\xi} = \tilde{\phi}(v - v_0(\xi,\eta))\left(\frac{\mathscr{T}_\nu + 1/2}{1 + \mathscr{J}/\mathscr{J}_{\mathrm{S}}} + \mathscr{S}\right) \tag{10}$$

where

$$\tilde{\phi} \equiv \phi\,\Delta v,$$

$$\mathscr{T}_\nu \equiv \frac{B}{A} I_\nu, \quad \mathscr{J} \equiv \frac{B}{A} J,$$

$$\mathscr{J}_{\mathrm{S}} \equiv \frac{P_{12} + P_{21} + 2C}{2A},$$

$$\mathscr{S} = \frac{P_{12} + P_{21} + 2C}{2(P_{12} - P_{21})}.$$

The great complexity of the problem derives from the term $\mathscr{J}$ that contains the contributions of all the rays propagating in all the possible directions: in other words, when we are integrating the radiative transfer equation, in each point $(\xi, \eta)$ we need to take into account all the maser photons passing through this point. This problem can be bypassed by means of the results cited in Sect. 4 that lead to the following conclusions:

1. at every point the strongest ray overwhelms the other ones;
2. in our Keplerian disk model the strongest ray is the one passing through the rotation center (see Fig. 4), with the only exception of the inner part of the disk where this ray has its minimum (see also the full line in Fig. 8); let us indicate this with $\mathscr{T}^{(0)}$.

Consequently the integral in $\mathscr{J}$ reduces to

$$\mathscr{J} \equiv \frac{1}{4\pi}\int_{4\pi} \mathscr{T}\,\mathrm{d}\Omega \simeq \frac{\Omega_{\mathrm{m}}}{4\pi}\max\{\mathscr{T}, \mathscr{T}^{(0)}\}$$





where $\mathscr{T} \equiv \int_0^{+\infty} \mathscr{T}_\nu \phi \mathrm{d}\nu$ and $\Omega_{\mathrm{m}}$ is the solid angle in which the maser emission is beamed. In our notation the $\mathscr{T}$ that appears in $\max\{\ldots\}$ is the ray along the line of sight [i.e. the ray we integrate in Eq. (10)].

As a further approximation we use $\mathscr{T}_\nu$ instead of $\mathscr{T}$: this should change slightly the line wings, without affecting the peak intensity; anyway the line profile is strongly determined by the function $\tilde{\phi}$, so that our approximation has little influence on it.

Now we can write the integral term as follows:

$$\frac{\mathscr{J}}{\mathscr{J}_{\mathrm{S}}} \simeq \max\{\mathscr{T}_\nu(\xi,\eta), \mathscr{T}^{(0)}(\mathscr{R})\}/\mathscr{T}_{\mathrm{S}}$$

with $\mathscr{T}_{\mathrm{S}} \equiv \frac{4\pi}{\Omega_{\mathrm{m}}}\mathscr{J}_{\mathrm{S}}$.

Actually for every ray one should include in the integration also the ray coming in the opposite direction (which is identical because of the symmetry of the problem), since in a saturated maser they strongly influence each other. There is no conceptual difficulty in taking care of this fact, but we decided to make such a distinction only for ray $\mathscr{T}^{(0)}$ in order to simplify the numerical integration.

In the following we indicate with $\mathscr{T}^{(0)-}$ and $\mathscr{T}^{(0)+}$ the two opposite rays.

### A.1. Full inversion

When the whole disk is masering, we have to solve the following system of ordinary differential equations:

$$\frac{\mathrm{d}\tilde{\mathscr{T}}_\nu}{\mathrm{d}\xi} = \tilde{\phi}(v - v_0(\xi,\eta))\left(\frac{\tilde{\mathscr{T}}_\nu + 1/(2\mathscr{T}_{\mathrm{S}})}{1 + \max\{\tilde{\mathscr{T}}_\nu, \tilde{\mathscr{T}}^{(0)}(\mathscr{R})\}} + \tilde{\mathscr{S}}\right) \tag{11}$$

$$\frac{\mathrm{d}\tilde{\mathscr{T}}^{(0)+}}{\mathrm{d}\mathscr{R}} = \tilde{\phi}(0)\left(\frac{\tilde{\mathscr{T}}^{(0)+} + 1/(2\mathscr{T}_{\mathrm{S}})}{1 + \tilde{\mathscr{T}}^{(0)+}(\mathscr{R}) + \tilde{\mathscr{T}}^{(0)+}(-\mathscr{R})} + \tilde{\mathscr{S}}\right) \tag{12}$$

with the initial conditions

$$\tilde{\mathscr{T}}_\nu(-\xi_0) = 0$$

$$\tilde{\mathscr{T}}^{(0)+}(-\mathscr{R}_0) = 0$$

and the definitions $\tilde{\mathscr{T}}_\nu \equiv \mathscr{T}_\nu/\mathscr{T}_{\mathrm{S}}$, $\tilde{\mathscr{T}}^{(0)\pm} \equiv \mathscr{T}^{(0)\pm}/\mathscr{T}_{\mathrm{S}}$, $\tilde{\mathscr{S}} \equiv \mathscr{S}/\mathscr{T}_{\mathrm{S}}$, $\xi_0 \equiv \sqrt{\mathscr{R}_0^2 - \eta^2}$ and $\tilde{\mathscr{T}}^{(0)} \equiv \tilde{\mathscr{T}}^{(0)+} + \tilde{\mathscr{T}}^{(0)-}$. As previously explained, we have used the symbols + and − to distinguish the rays propagating along the same path, but in opposite directions. In Eq. (12) $\mathscr{R}$ has to be regarded as a variable ranging in the intervals $-\mathscr{R}_0 < \mathscr{R} < -\mathscr{R}_{\mathrm{m}}$, $\mathscr{R}_{\mathrm{m}} < \mathscr{R} < \mathscr{R}_0$. The second equation is equal to the first one evaluated in $\eta = 0$ and $v = \nu_{\mathrm{H_2O}}$. We have not averaged (12) over the line profile (as done by Alcock and Ross, 1985a) since it can introduce only a factor $\sim 1$ in the equation.

It is a must to underline that we have also made use of the special symmetry of the problem to express Eq. (12) by means of $\tilde{\mathscr{T}}^{(0)+}$ only: in fact it is

$$\tilde{\mathscr{T}}^{(0)-}(\mathscr{R}) = \tilde{\mathscr{T}}^{(0)+}(-\mathscr{R}).$$

In this form it can be solved with a simple iterative algorithm. After that it is straightforward to compute $\tilde{\mathscr{T}}^{(0)}$ and solve Eq. (11) numerically.

In order to perform the numerical integration we have to give suitable values to the parameters used.

A rough estimate of $\mathscr{T}_{\mathrm{S}}$ can be given using the value $T_{\mathrm{S}} \simeq 10^{11}$ K (Genzel, 1985) for the brightness saturation temperature of $H_2O$ masers:

$$\mathscr{T}_{\mathrm{S}} = \frac{B}{A} I_{\mathrm{S}} \equiv \frac{c^2}{2h\nu_{\mathrm{H_2O}}^3}\,\frac{2k\nu_{\mathrm{H_2O}}^2}{c^2}\, T_{\mathrm{S}} \simeq 10^{11}.$$

Reasonable estimates for other parameters may be taken from Alcock and Ross (1985a) and Goldreich and Keeley (1972), that suggest $\mathscr{S} \simeq 10 - 10^3$ and $L \simeq 10^{12} - 10^{14}$ cm so that we can choose

$$\tilde{\mathscr{T}} = 10^{-9};\ L = 10^{14}\ \mathrm{cm} \to \mathscr{R}_0 = 10^2$$

for a disk with $R_0 \simeq 10^{16}$ cm (Elmegreen and Morris, 1979).

The inner radius $R_{\mathrm{m}}$, the line width $\Delta v$ and the minimum rotation velocity $v_0$ have been deduced from the observed spectra using the criteria explained in Sect. 3: $R_{\mathrm{m}} = 0.4\, R_0$, $\Delta v = 59$ kHz, $v_0 = 4.5\ \mathrm{km\,s^{-1}}$.

### A.2. Partial inversion

Here we consider a disk with quenched inversion in a given sector, described by inequality (3). Now Eq. (11) takes the form:

$$\frac{\mathrm{d}\tilde{\mathscr{T}}_\nu}{\mathrm{d}\xi} = \begin{cases} 0 & \text{if } \beta\eta < \xi < -\beta\eta, \\ \tilde{\phi}(v - v_0(\xi,\eta))\left[\left(\dfrac{\tilde{\mathscr{T}}_\nu + 1/(2\mathscr{T}_{\mathrm{S}})}{1 + \max\{\tilde{\mathscr{T}}_\nu, \tilde{\mathscr{T}}^{(1)}(\mathscr{R})\}}\right) + \tilde{\mathscr{T}}\right] & \\ \tilde{\phi}(v - v_0(\xi,\eta))\left[\left(\dfrac{\tilde{\mathscr{T}}_\nu + 1/(2\mathscr{T}_{\mathrm{S}})}{1 + \max\{\tilde{\mathscr{T}}_\nu, \tilde{\mathscr{T}}^{(0)}(\mathscr{R})\}}\right) + \tilde{\mathscr{T}}\right] & \text{if } -\beta\eta < \xi < \beta\eta, \\ & \text{elsewhere,} \end{cases}$$

where $\tilde{\mathscr{T}}_\nu(-\xi_0) = 0$, $\tilde{\mathscr{T}}^{(0)}$ is the same of Eq. (12) and $\tilde{\mathscr{T}}^{(1)}$ is given just by Eq. (12) integrated between $\mathscr{R}_{\mathrm{m}}$ and $\mathscr{R}_0$, with the condition $\tilde{\mathscr{T}}^{(1)+}(\mathscr{R}_{\mathrm{m}}) = 0$. The comparison between these two rays is shown in Fig. 8, where $\tilde{\mathscr{T}}^{(0)}$ is represented by the full line and $\tilde{\mathscr{T}}^{(1)}$ by the dashed one.

Of course in the limit $\beta = 0$ we obtain the same results of Sect. A.1.

### References


Alcock, C., Ross, R.R.: 1985a, *Astrophys. J.* **290**, 433
Alcock, C., Ross, R.R.: 1985b, *Astrophys. J.* **299**, 763
Barvainis, R.: 1984, *Astrophys. J.* **279**, 358
Cesaroni, R., Palagi, F., Felli, M., Catarzi, M., Comoretto, G., Di Franco, S., Giovanardi, C., Palla, F.: 1988, *Astron. Astrophys. Suppl.* **76**, 445
Comoretto, G., Palagi, F., Cesaroni, R., Felli, M., Bettarini, A., Catarzi, M., Curioni, G.P., Curioni, P., Di Franco, S., Giovanardi, C., Massi, M., Palla, F., Panella, D., Rossi, E., Speroni, N., Tofani, G.: 1990, *Astron. Astrophys. Suppl.* (in press)
Elitzur, M.: 1982, *Rev. Mod. Phys.* **54**, 1225
Elmegreen, B.G., Morris, M.: 1979, *Astrophys. J.* **229**, 593
Genzel, R.: 1985, in *Masers, Molecules and Mass outflows in Star Forming Regions*, ed. A.D. Haschick, Haystack Observatory, Westford, p. 233
Genzel, R., Downes, D.: 1977, *Astron. Astrophys. Suppl.* **30**, 145
Genzel, R., Reid, M.J., Moran, J.M., Downes, D.: 1981, *Astrophys. J.* **244**, 884
Grinin, V.P., Grigor'ev, S.A.: 1983a, *Sov. Astron.* **27**, 298
Grinin, V.P., Grigor'ev, S.A.: 1983b, *Sov. Astron. Lett.* **9**, 244

Postdoc at Arcetri
(2006)

# Source 1: S255

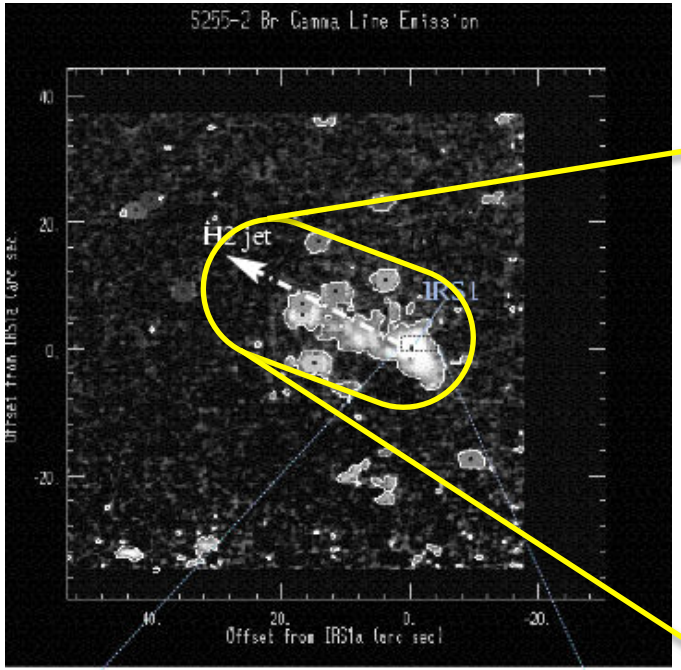


L~$10^4$ $L_\odot$, B1

$M_{dyn}$~15 $M_\odot$

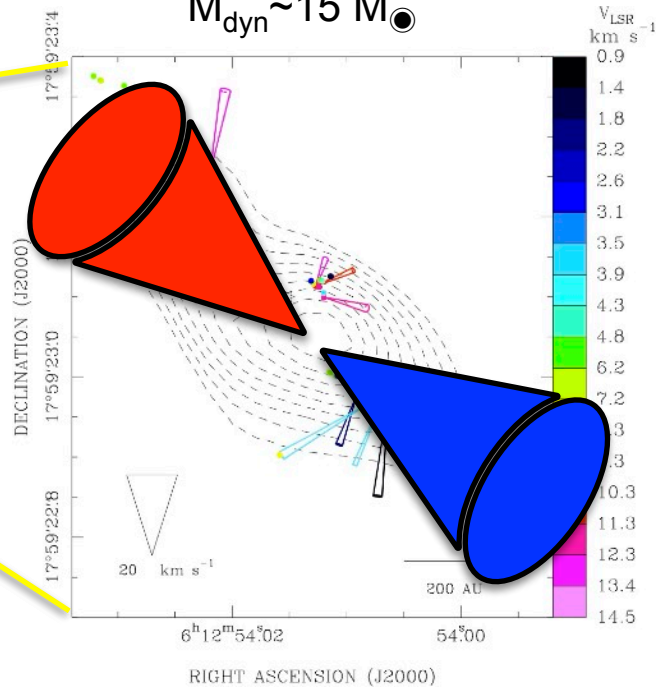


- Brackett Gamma (grayscale map)
- 15 GHz Radio continuum (contours)
- Water maser proper motions (Arrows)

Outflow not disk!

Goddi, Moscadelli, Sanna, Cesaroni and Minier 2007

# Source 1: S255

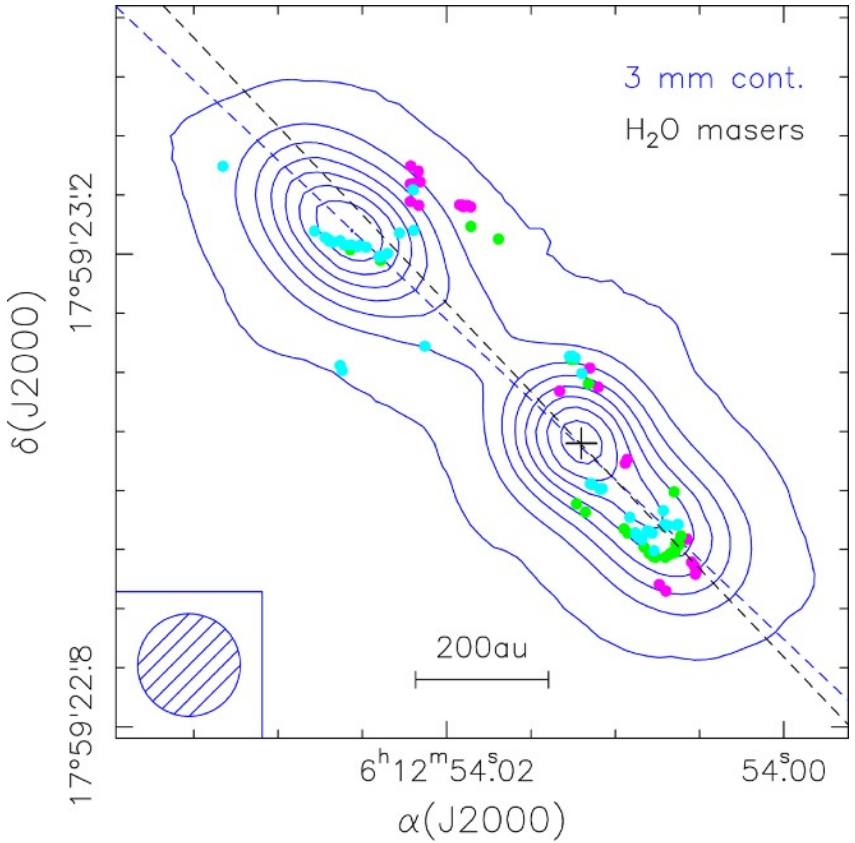


A&A 612, A103 (2018)

## Radio outburst from a massive (proto)star

### When accretion turns into ejection★

R. Cesaroni[1], L. Moscadelli[1], R. Neri[2], A. Sanna[3], A. Caratti o Garatti[4], J. and C. M. Walmsley★★

Cesaroni et al.,

2018

2023

2025

# Source 2: G24.78+0.08 A1

## *Wide-angle outflow from $H_2O$ masers*

D~7.7kpc, L~7×10⁴ $L_\odot$

O9.5 star, 20 $M_\odot$

Rotating toroid from
a dense molecular core

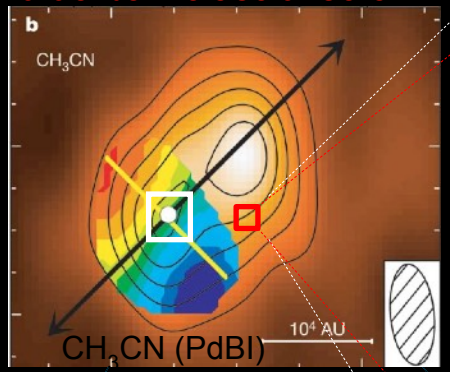


Beltran, Cesaroni, et al. 2005

*Rotatir*

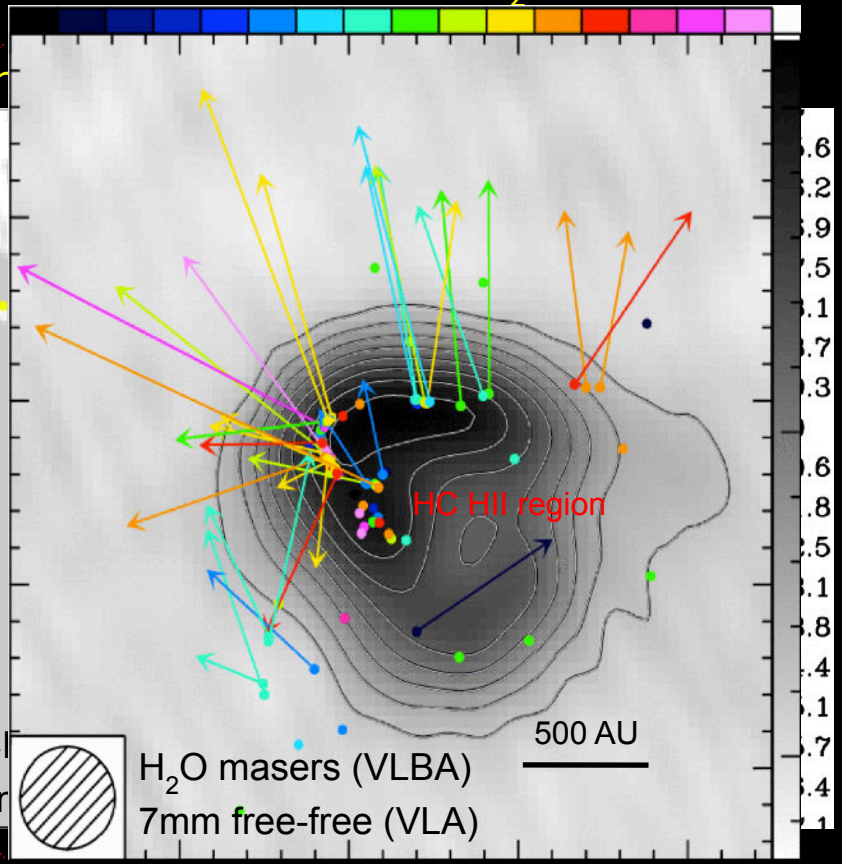


Large scales:

HC-HII reg. is confined by a molec. (rotating/infalling) toroid

Small scales:

The HC HII may be expanding based on $H_2O$ masers

Open Q at that time:
Has accretion onto the central star(s) ended?

*Beltran, Cesaroni et al. 2006*
*Moscadelli, Goddi, Cesaroni, et al. (2007)*

# Postdoc at the CfA (2006-2009)

# Orion

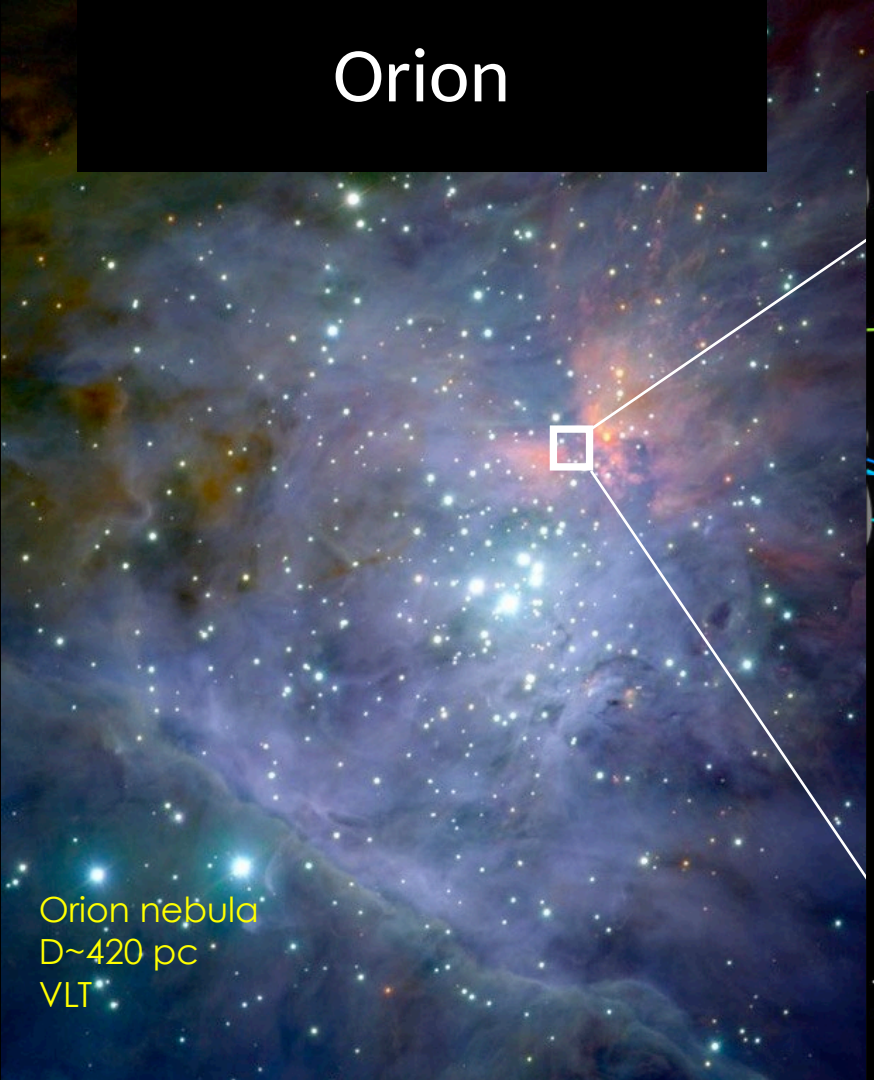
Orion nebula
D~420 pc
VLT

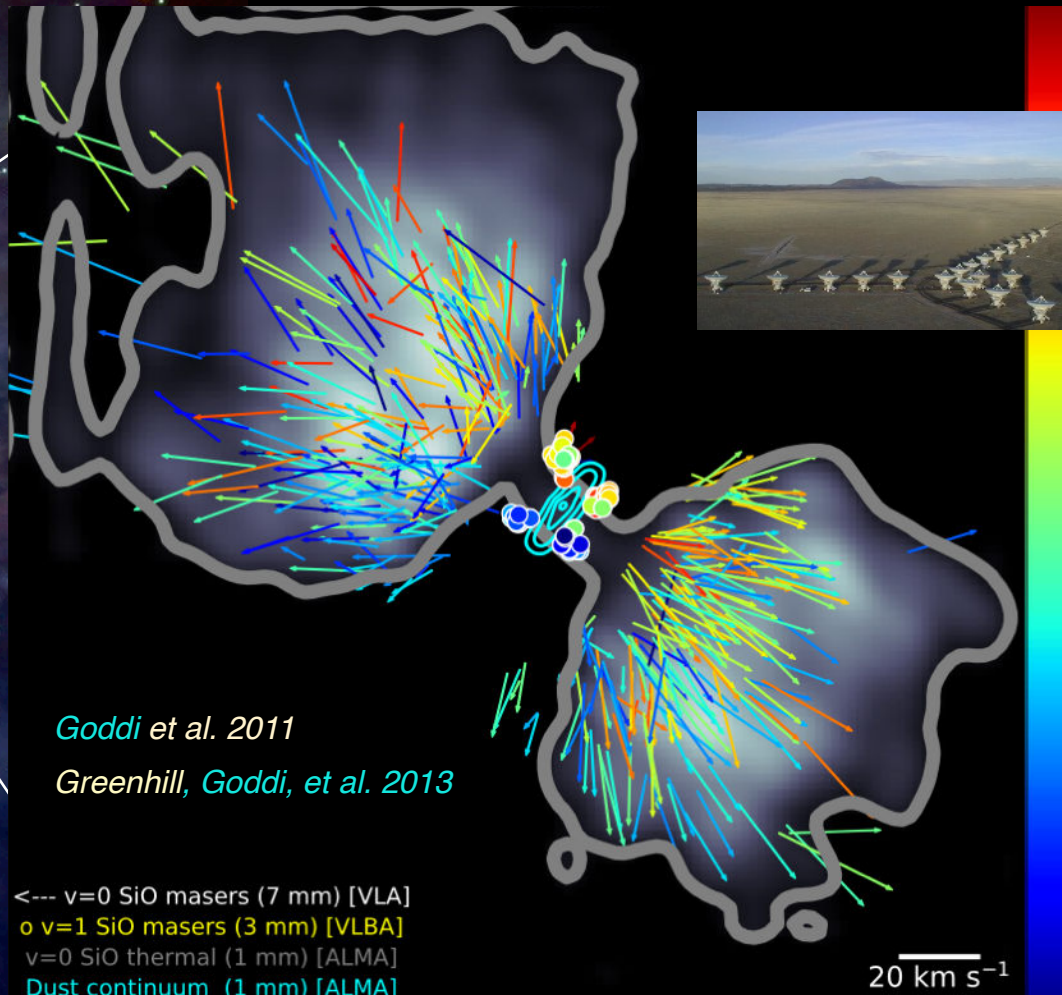
Goddi et al. 2011
Greenhill, Goddi, et al. 2013
<--- v=0 SiO masers (7 mm) [VLA]
o v=1 SiO masers (3 mm) [VLBA]
v=0 SiO thermal (1 mm) [ALMA]
Dust continuum (1 mm) [ALMA]
20 km s$^{-1}$

7 mm continuum (Mar 31, 2002)
7 mm SiO masers (2001-2002 monitoring)
3 mm SiO masers (Jan 24, 2011)

Wide-angle outflow

Rotation axis

Disk mid-plane

Wide-angle outflow

Wide-angle outflow

20 AU

Wide-angle outflow

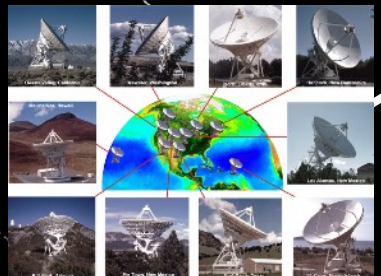

20 km s$^{-1}$

*Matthews, Greenhill, Goddi, et al. 2010*

*Issaoun, Goddi, et al. 2017*

# The most detailed view of a disk-wind from a massive YSO

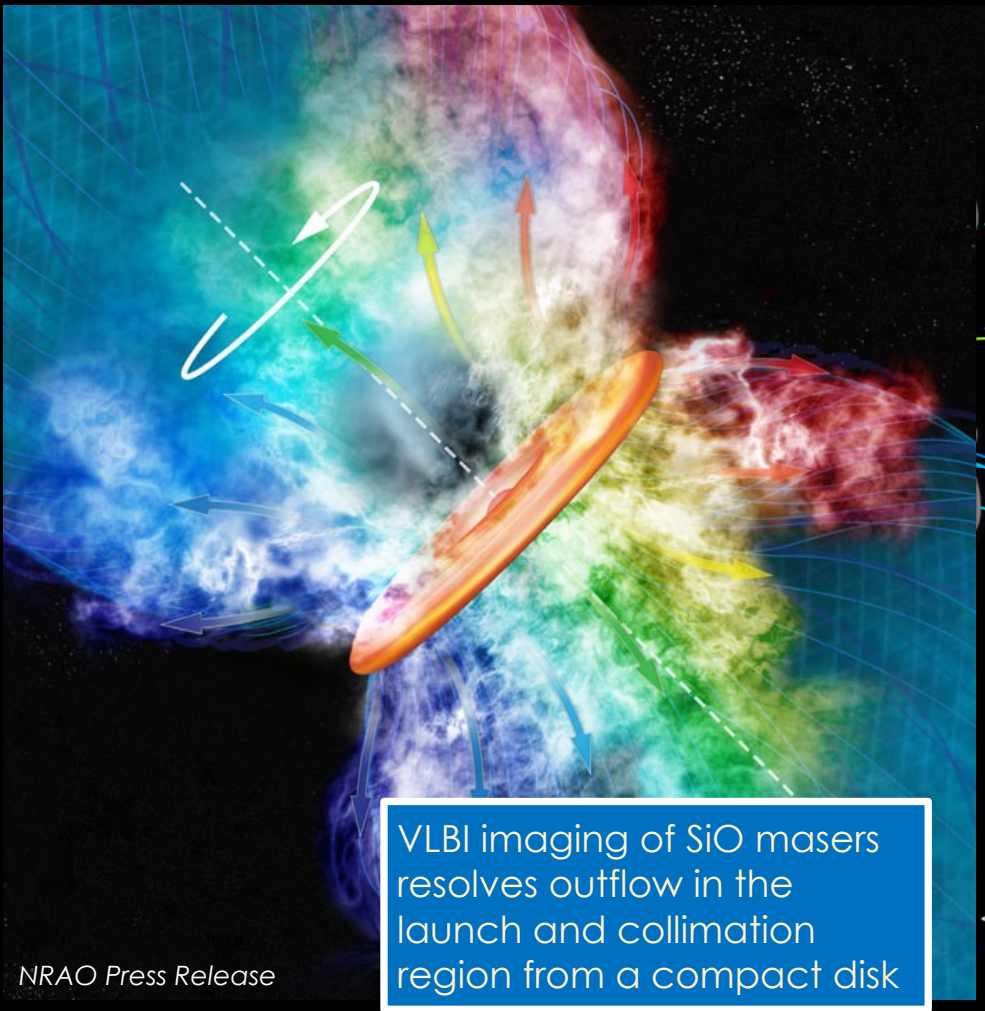

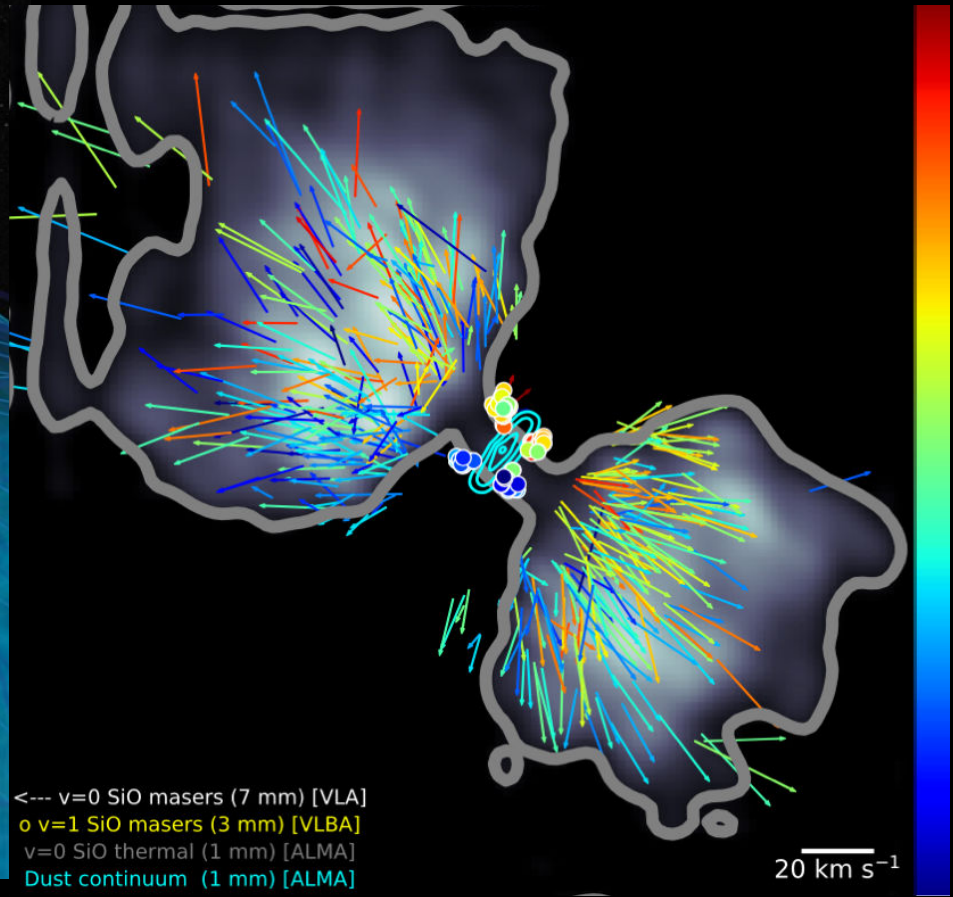


VLBI imaging of SiO masers resolves outflow in the launch and collimation region from a compact disk

*NRAO Press Release*

A beautiful Keplerian Disk around a ~ 15 $M_\odot$ YSO

Orion Source I

ALMA Cycle V Band 6 Beamsize ~0.02-0.05”

Length ~ 90 AU, Height ~35 AU

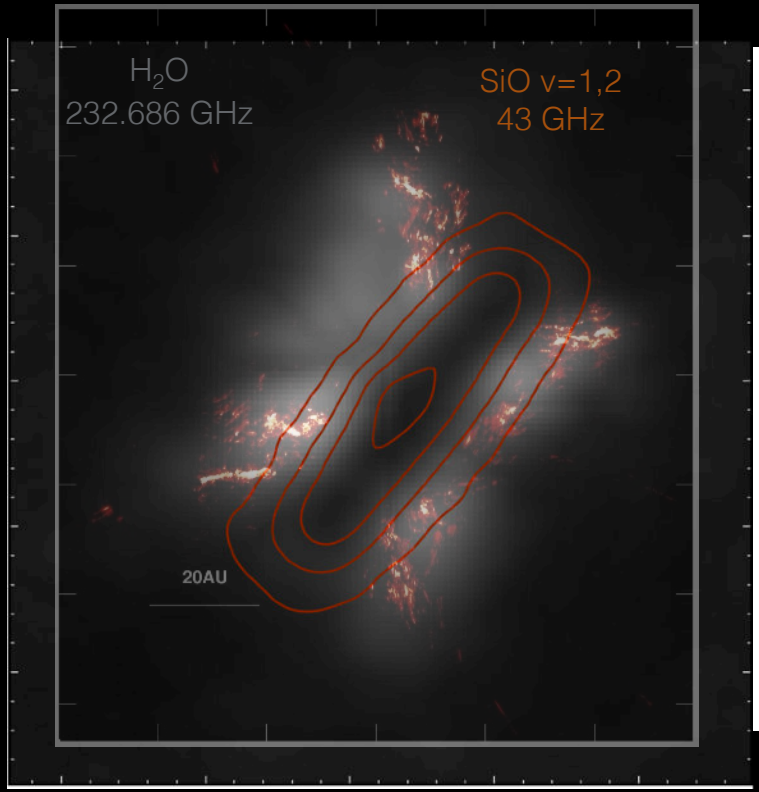


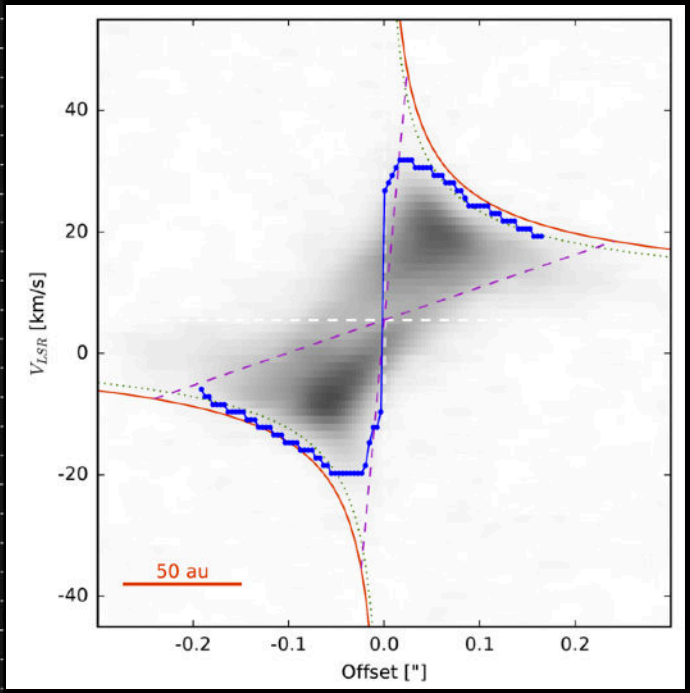


*Ginsburg, Bally, Goddi, Wright, Plambeck 2018*

# 2011-2013

ALMA Early Science, Massive Star Formation workshop

ESO Garching, 8 April, 2011

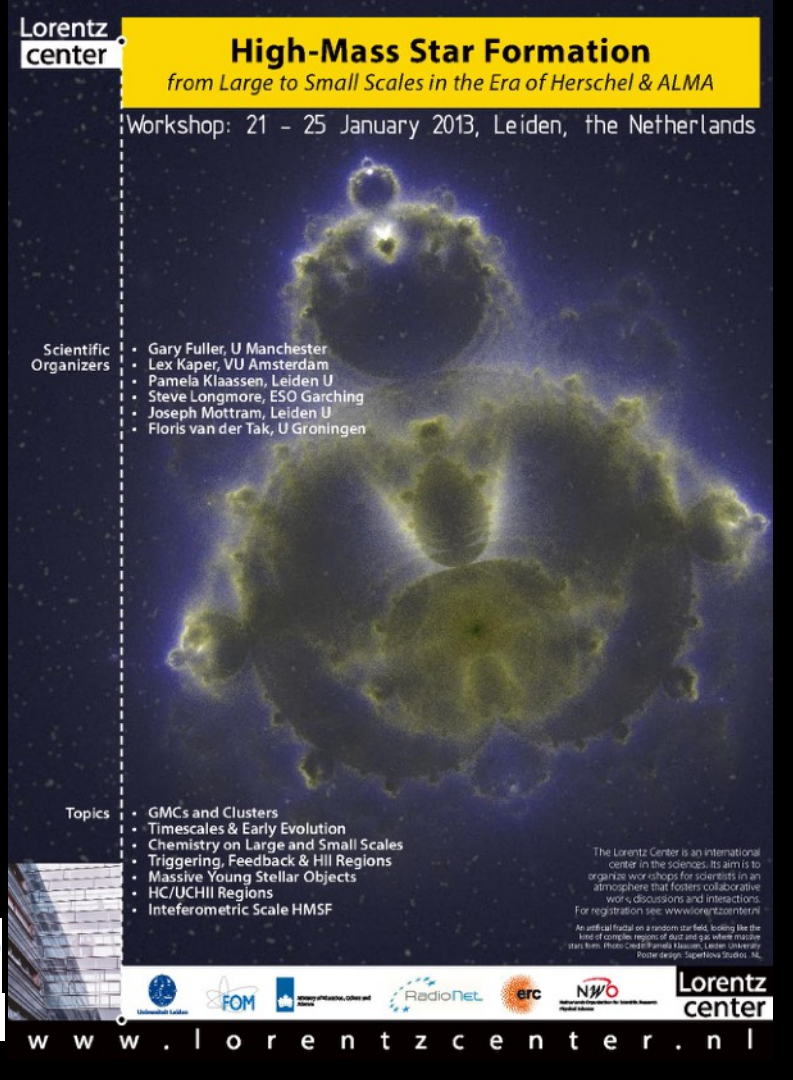

A&A 602, A59 (2017)
DOI: 10.1051/0004-6361/201630184


Astronomy & Astrophysics

# Chasing discs around O-type (proto)stars: Evidence from ALMA observations

R. Cesaroni[1], Á. Sánchez-Monge[2], M. T. Beltrán[1], K. G. Johnston[3], L. T. Maud[4], L. Moscadelli[1], J. C. Mottram[5], A. Ahmadi[5], V. Allen[6], H. Beuther[5], T. Csengeri[7], S. Etoka[8], G. A. Fuller[9,10], D. Galli[1], R. Galván-Madrid[11], C. Goddi[12,4], T. Henning[5], M. G. Hoare[13], P. D. Klaassen[14], R. Kuiper[15], M. S. N. Kumar[16,17], S. Lumsden[18], T. Peters[19], V. M. Rivilla[1], P. Schilke[2], L. Testi[20,1], F. van der Tak[21,6], S. Vig[22], C. M. Walmsley[23,1], and H. Zinnecker[24]

*(Affiliations can be found after the references)*

Received 2 December 2016 / Accepted 30 January 2017



**Table 1.** Targets for the ALMA observations with their main parameters, obtained from the literature.

| Name | Other names | $\alpha$(J2000) (h m s) | $\delta$(J2000) (° ′ ″) | $V_{\rm LSR}$ (km s$^{-1}$) | $d$ (kpc) | $L_{\rm bol}$ ($10^5$ $L_\odot$) | $M_{\rm gas}$[a] ($10^3$ $M_\odot$) | Ref.[c] |
|---|---|---|---|---|---|---|---|---|
| G17.64+0.16 | AFGL 2136 | 18 22 26.370 | −13 30 12.00 | 22.5 | 2.2 | 1.0 | 0.20 | 1 |
| G24.78+0.08 | | 18 36 12.661 | −07 12 10.15 | 111.0 | 7.7 | 2.2 | 4.8 | 2, 3 |
| G29.96−0.02 | W43 S | 18 46 03.665 | −02 39 22.00 | 98.0 | 5.26 | 5.8 | 1.3 | 4, 5 |
| G31.41+0.31 | | 18 47 34.315 | −01 12 45.90 | 96.5 | 7.9 | 2.6 | 5.2 | 3, 6 |
| G345.49+1.47 | | 16 59 41.610 | −40 03 43.30 | −12.6 | 2.4[b] | 1.5 | 1.2 | 1 |
| G345.50+0.35 | | 17 04 22.870 | −40 44 23.50 | −17.8 | 2.0 | 1.0 | 0.55 | 1 |

A&A 616, A66 (2018)
https://doi.org/10.1051/0004-6361/201832680


Astronomy & Astrophysics

# The feedback of an HC HII region on its parental molecular core

## The case of core A1 in the star-forming region G24.78+0.08

L. Moscadelli[1], V. M. Rivilla[1], R. Cesaroni[1], M. T. Beltrán[1], Á Sánchez-Monge[2], P. Schilke[2], J. C. Mottram[3], A. Ahmadi[3], V. Allen[4,5], H. Beuther[3], T. Csengeri[6], S. Etoka[7], D. Galli[1], C. Goddi[8,9], K. G. Johnston[10], P. D. Klaassen[11], R. Kuiper[12], M. S. N. Kumar[13,14], L. T. Maud[8], T. Möller[2], T. Peters[15], F. Van der Tak[4,5], and S. Vig[16]

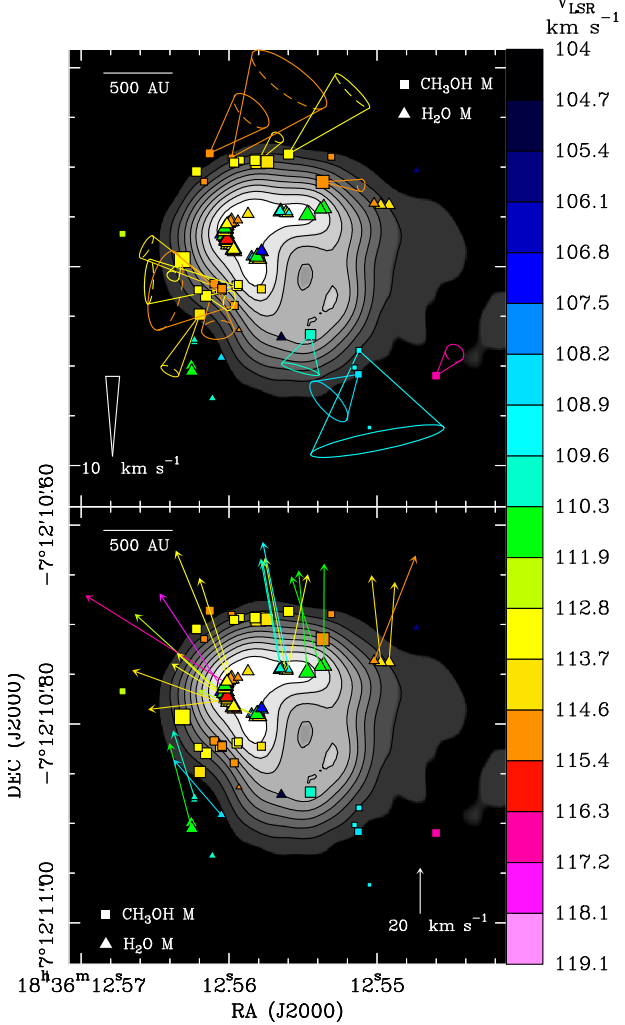


From the abstract:

*Over core A1, the $V_{LSR}$ maps from both the 1.4 mm molecular lines and the 6.7 GHz methanol masers consistently show a $V_{LSR}$ gradient directed approximately S–N. Rather than gravitationally supported rotation of a massive toroid,* ***we interpret this velocity gradient as a relatively slow expansion of core A1****.*

# Hot ammonia around young O-type stars

## I. JVLA imaging of $NH_3$ (6, 6) to (14, 14) in NGC 7538 IRS1

C. Goddi[1], Q. Zhang[2], and L. Moscadelli[3]

A&A 589, A44 (2016)
DOI: 10.1051/0004-6361/201527855


Astronomy & Astrophysics

## Hot ammonia around young O-type stars

### III. High-mass star formation and hot core activity in W51 Main⋆

C. Goddi[1,2], A. Ginsburg[3], and Q. Zhang[4]

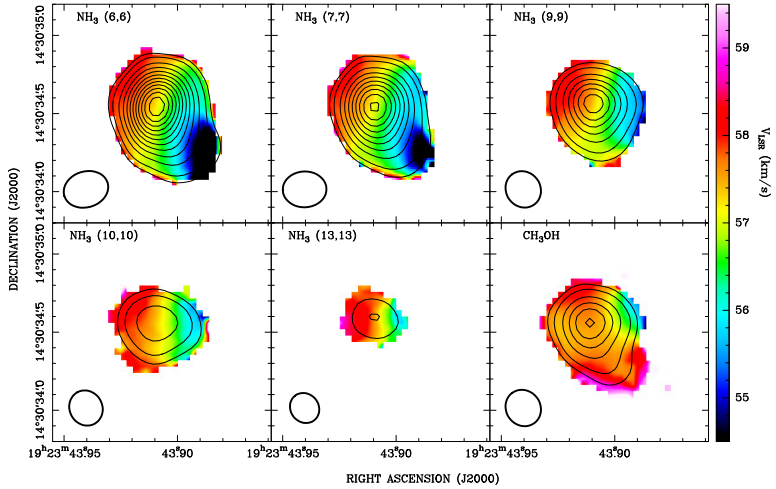


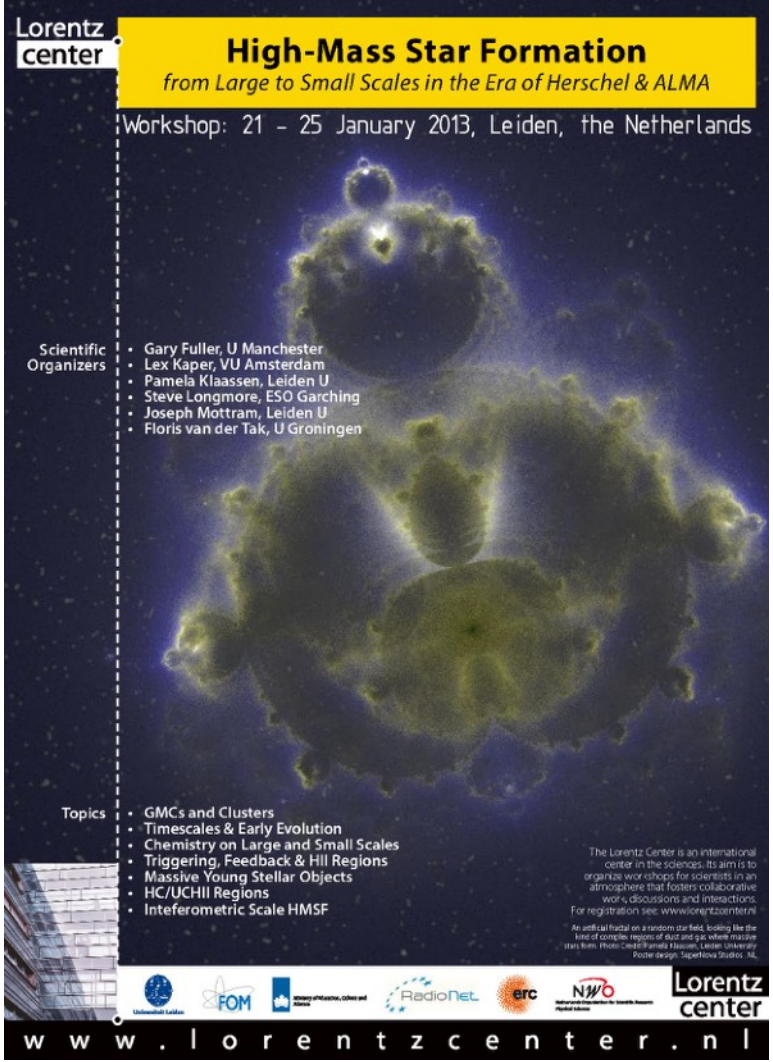

# W51 Star Forming Complex

$L \sim 10^7\ L_\odot$, D = 5.4 kpc

$M_{H2} > 10^5\ M_\odot$ in r < 2.5 pc

$M_* \sim 10^4\ M_\odot$ (~20 O-stars)

*Ginsburg, Goddi, et al. 2017*
*Goddi, Ginsburg et al. 2020*
*Yoon, Ginsburg,…Goddi,… et al. 2025*

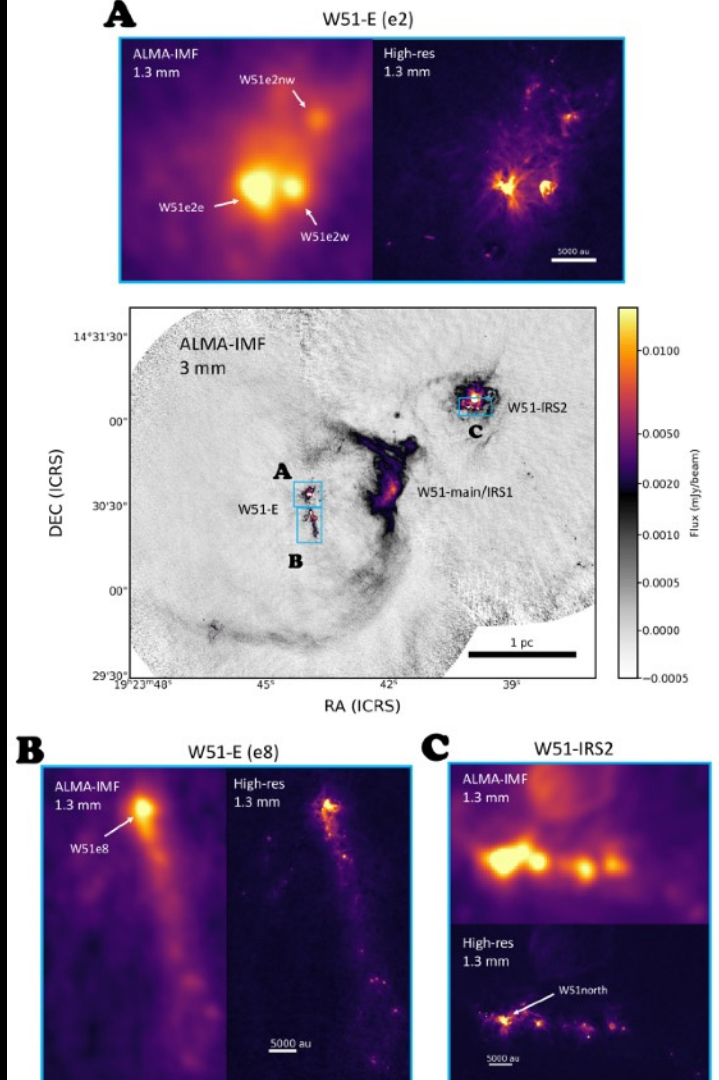

# Open Questions

1. Does the feedback from O-type YSOs halt SF?
2. Do “switched-on” O-stars keep accreting?
3. Do proto-O-stars accrete their mass via disks?

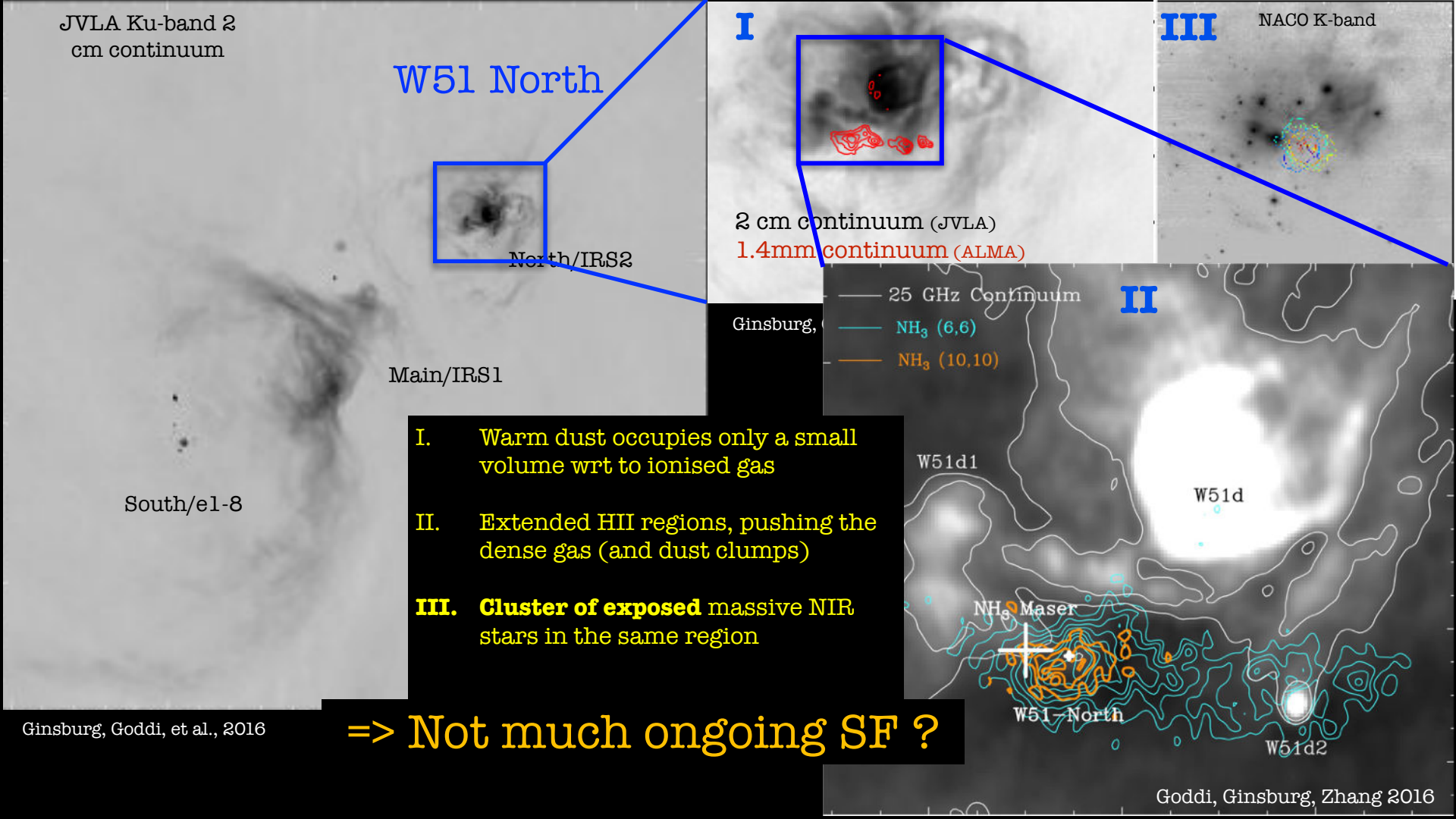
JVLA Ku-band 2 cm continuum
W51 North
North/IRS2
Main/IRS1
South/e1-8
Ginsburg, Goddi, et al., 2016
I
2 cm continuum (JVLA)
1.4mm continuum (ALMA)
Ginsburg,
III
NACO K-band
II
25 GHz Continuum
NH3 (6,6)
NH3 (10,10)
W51d1
W51d
NH3 Maser
W51-North
W51d2
Goddi, Ginsburg, Zhang 2016
I. Warm dust occupies only a small volume wrt to ionised gas
II. Extended HII regions, pushing the dense gas (and dust clumps)
III. Cluster of exposed massive NIR stars in the same region
=> Not much ongoing SF ?

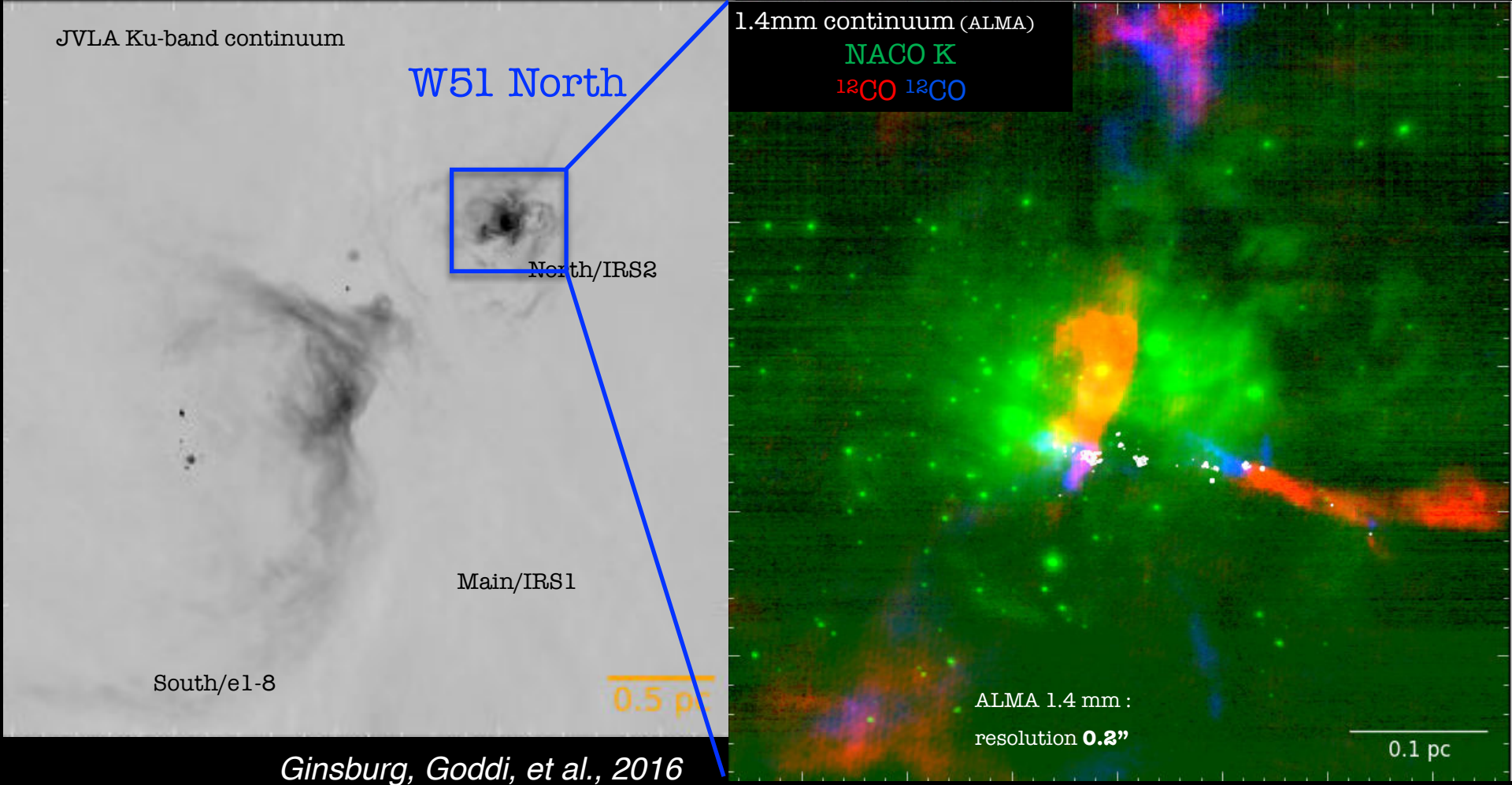


*Ginsburg, Goddi, et al., 2016*

*Ginsburg, Goddi, et al., 2017*

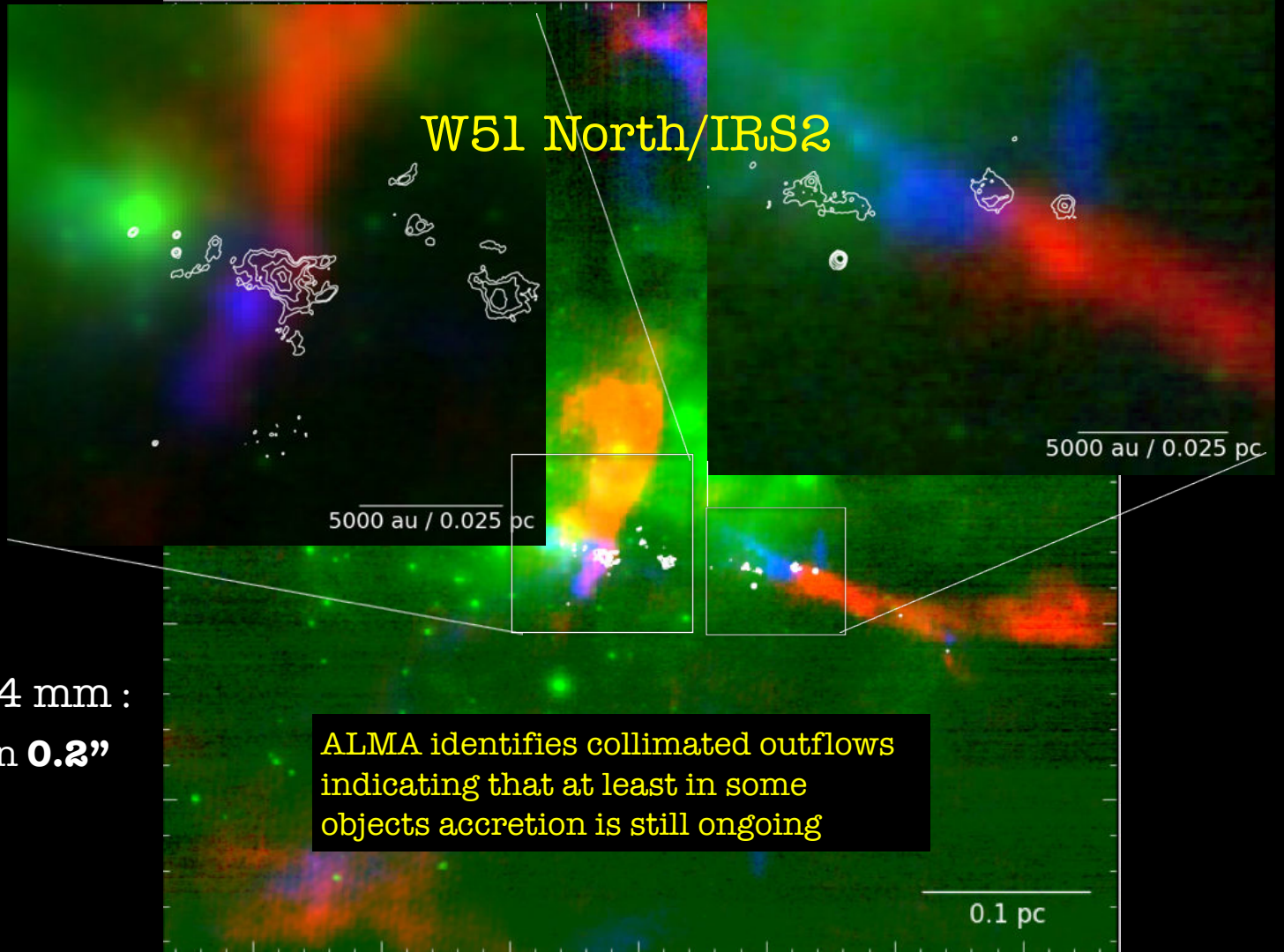


ALMA 1.4 mm :
resolution **0.2”**

ALMA identifies collimated outflows indicating that at least in some objects accretion is still ongoing

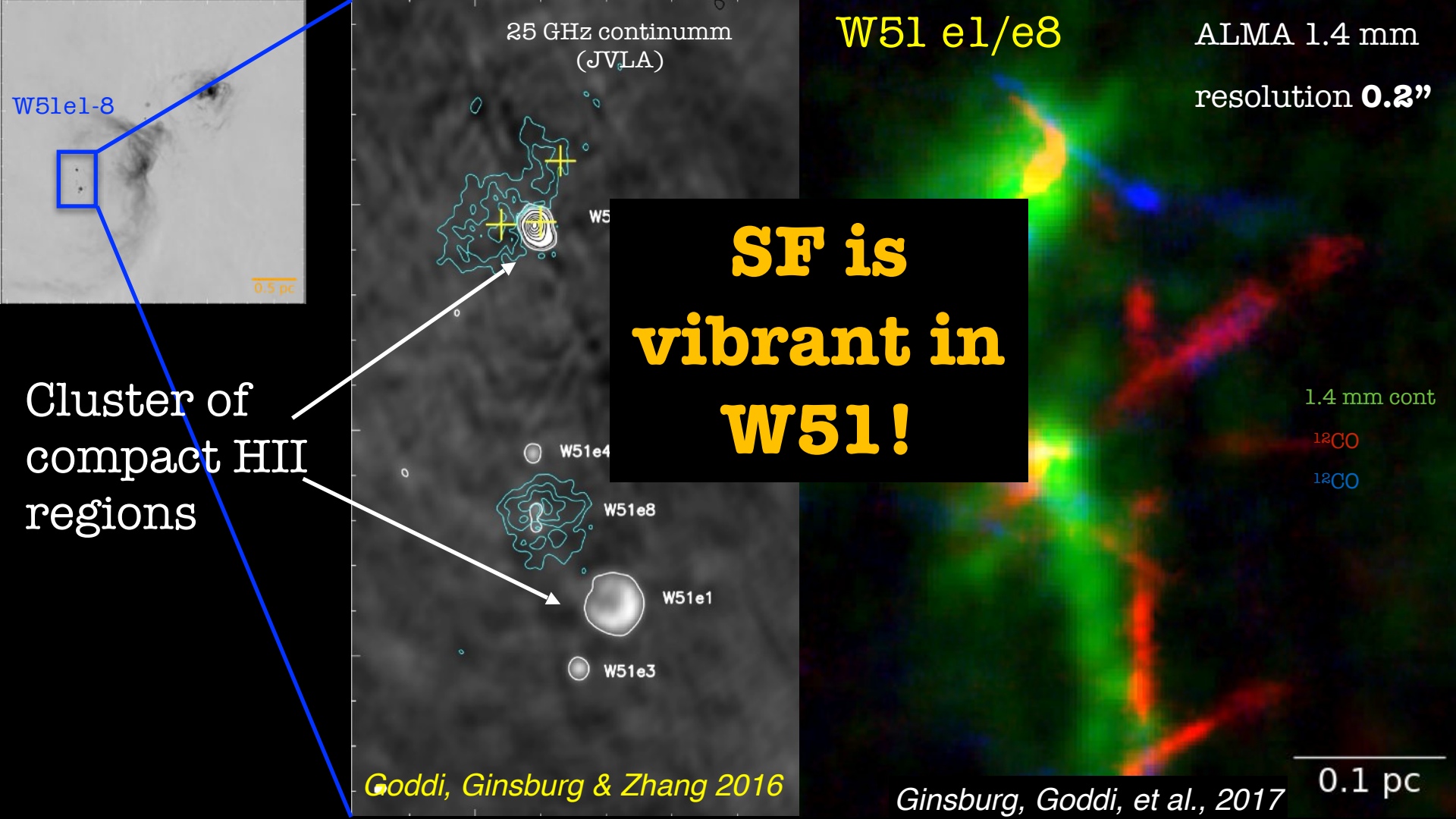
W51el-8
0.5 pc
25 GHz continumm
(JVLA)
W5
W51e4
W51e8
W51e1
W51e3
Goddi, Ginsburg & Zhang 2016
W51 e1/e8
ALMA 1.4 mm
resolution 0.2”
SF is vibrant in W51!
Cluster of compact HII regions
1.4 mm cont
12CO
12CO
Ginsburg, Goddi, et al., 2017
0.1 pc

# Q1: Does the feedback from O-type YSOs halt SF?

NO

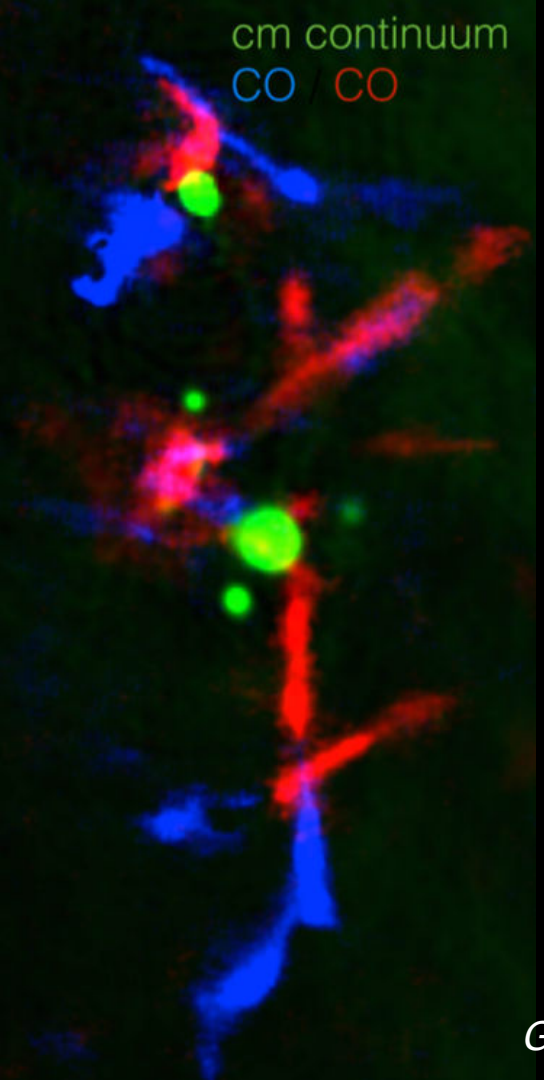


## Which sources are driving these multiple collimated outflows?

None of the outflows come from the HII regions

Q2: Do “switched-on” O-stars keep accreting?

NO

*Ginsburg, Goddi, et al., 2017*

# Q3: Do proto-O-stars accrete their mass via disks?

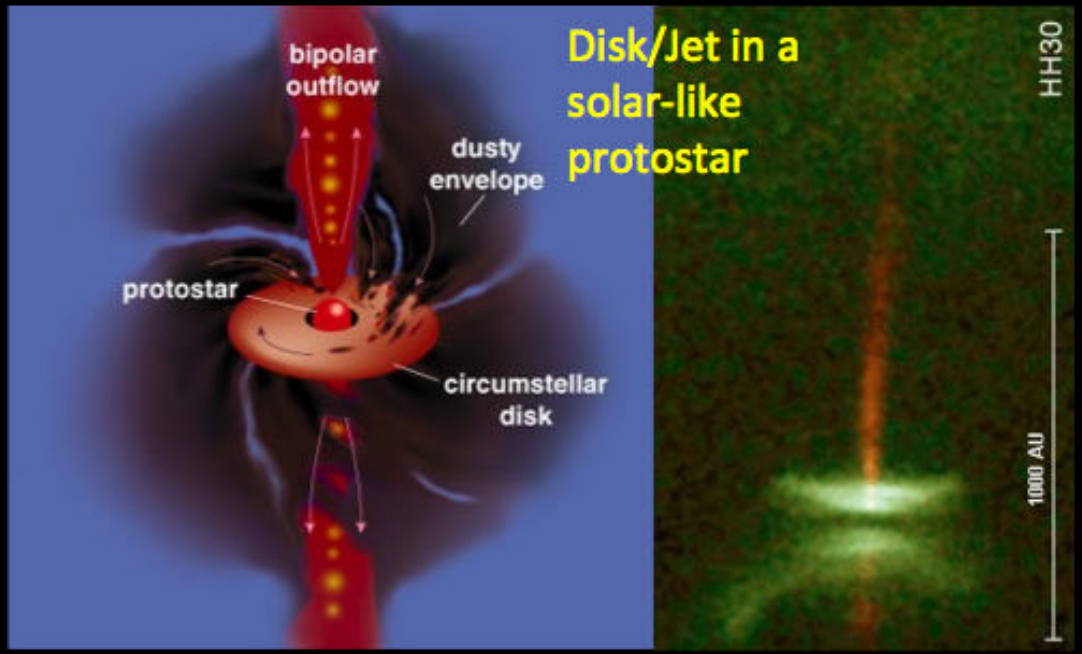


We used ALMA to map the outflows at high angular resolution and look for disks

# Finding 1: Collimated outflows from dusty sources

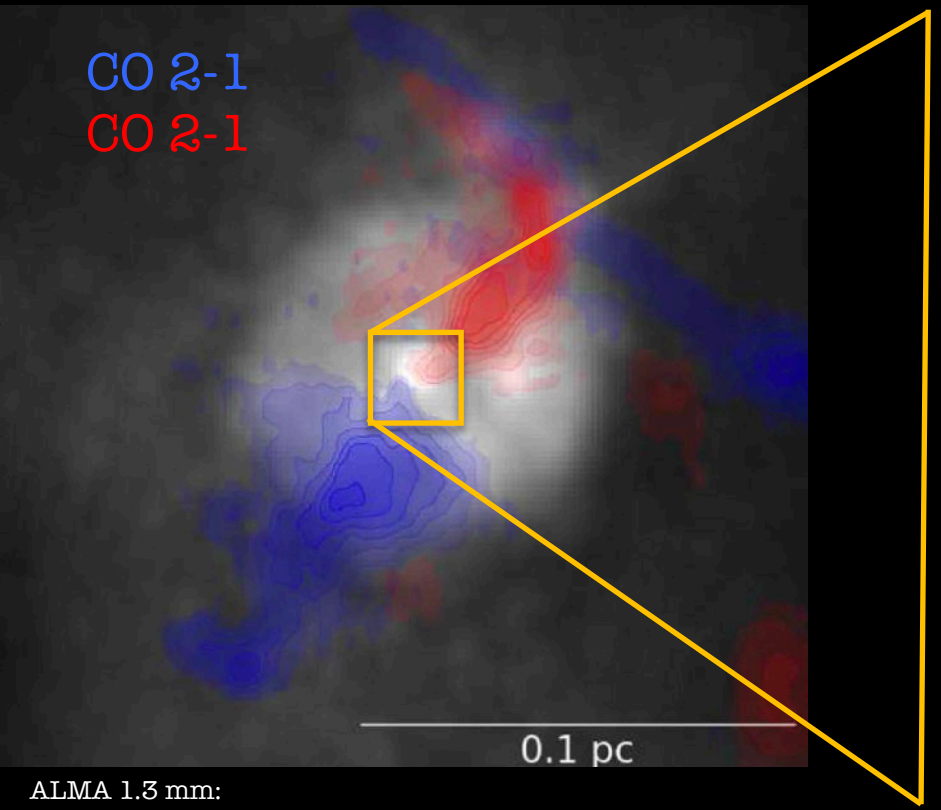


ALMA 1.3 mm:

**0.2”** ang. res.

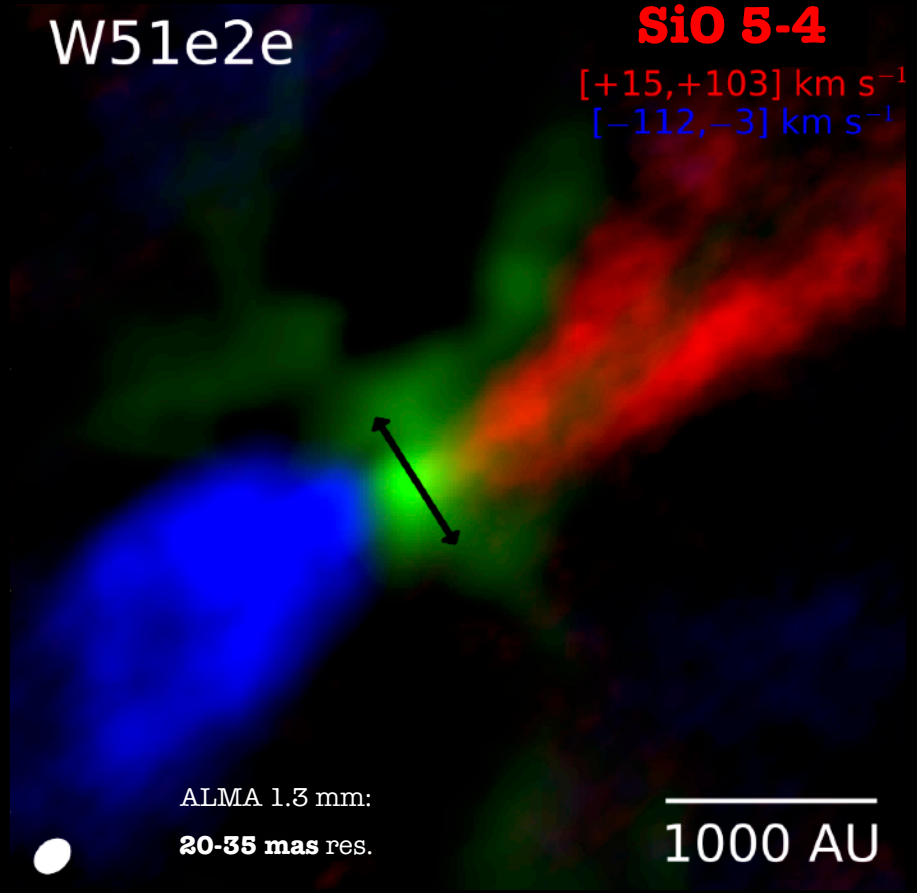


ALMA 1.3 mm:

**20-35 mas** res.

*Goddi, et al. 2020*

# *Finding 1: Collimated outflows from dusty sources*

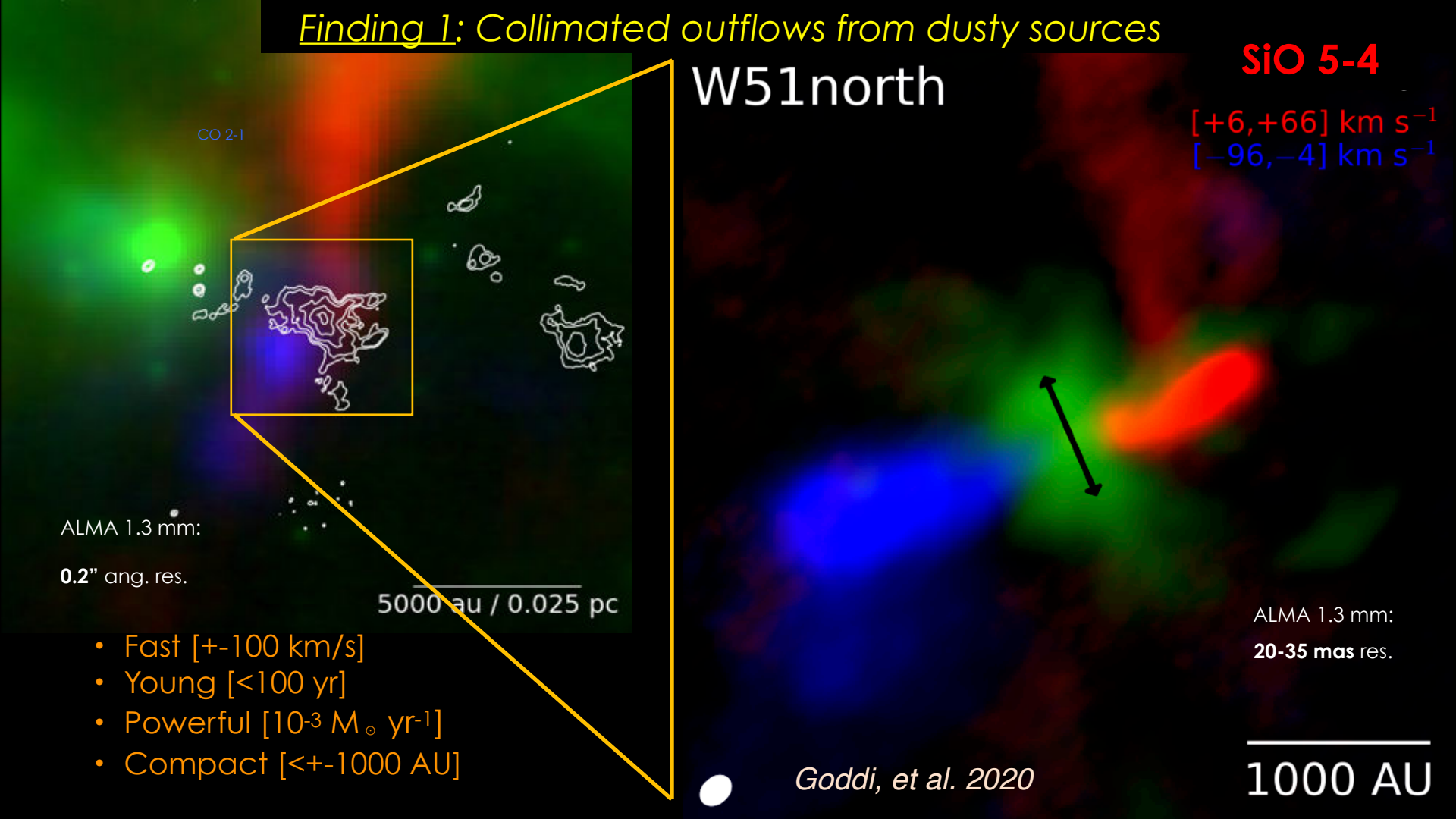


- Fast [+-100 km/s]
- Young [<100 yr]
- Powerful [$10^{-3}$ $M_\odot$ $yr^{-1}$]
- Compact [<+-1000 AU]

*Goddi, et al. 2020*

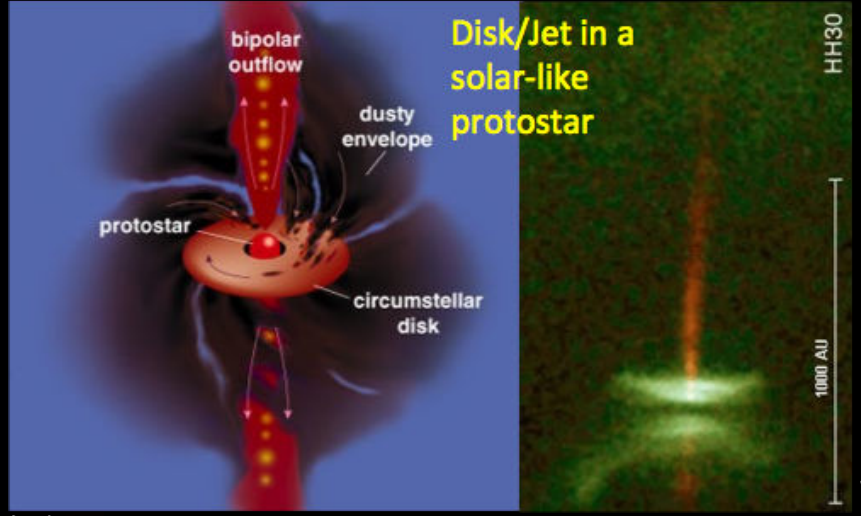


W51e2e

Full-Velocity
[+15,+103] km s$^{-1}$
[−112,−3] km s$^{-1}$

1000 AU

Are we finally seeing disk/jet systems similar to solar-like stars?

W51north

Full-Velocity
[+6,+66] km s$^{-1}$
[−96,−4] km s$^{-1}$

1000 AU

# Finding 2: Morphology of the mm dust emission continuum

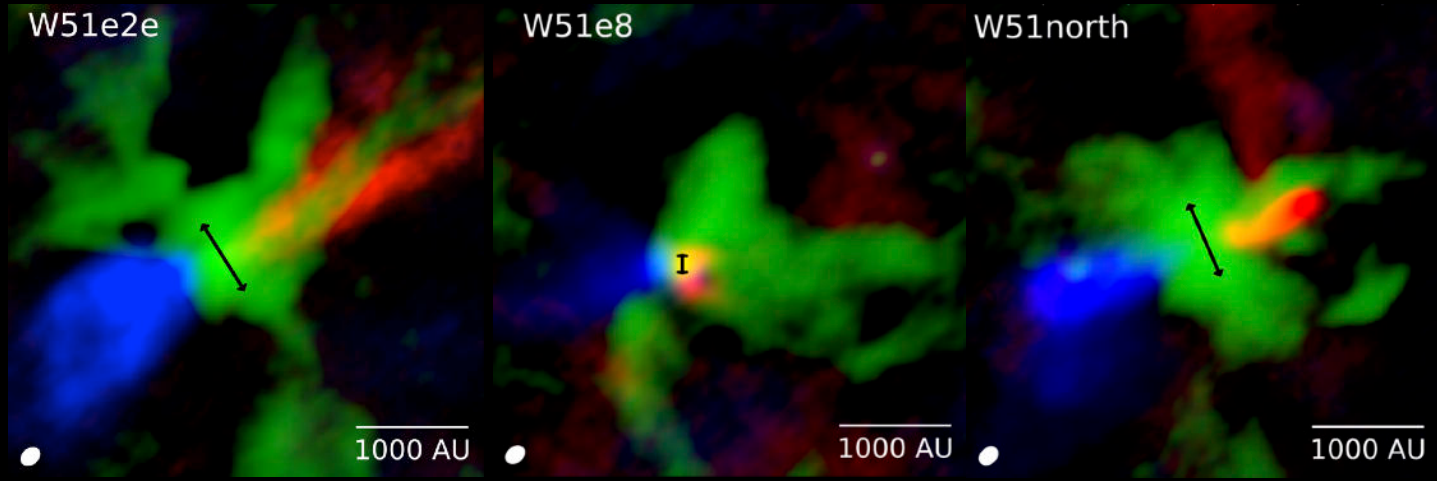


Goddi, et al. 2020

Continuum (green) does not show a simple flattened structure at the center of the outflows, but the emission is resolved into multiple dusty lanes converging onto the compact cores

Mass (and angular momentum) conveyed to the star via multiple channels?

# Finding 3: Outflow from W51-north has different P.A. on different scales

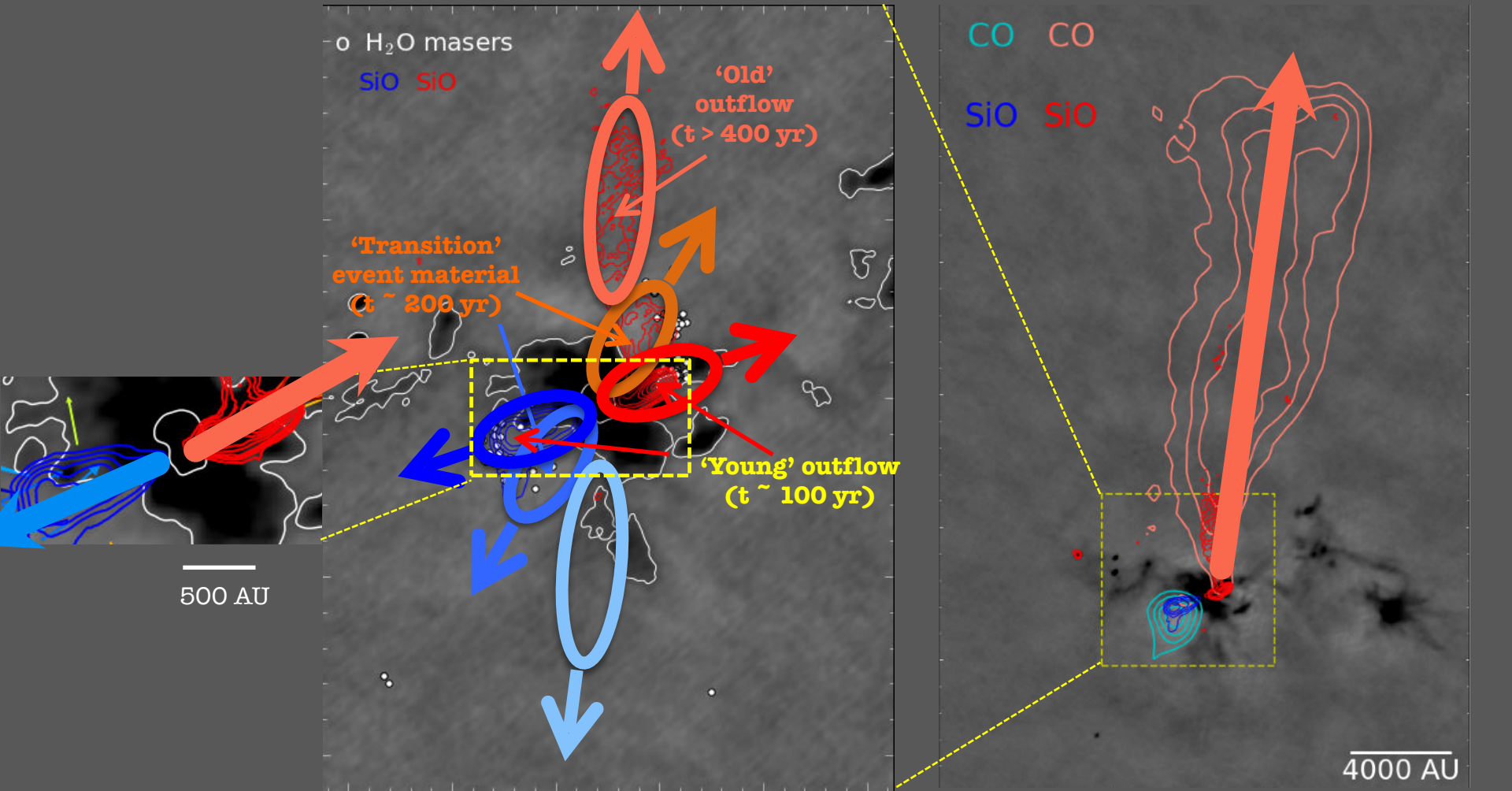

National Radio Astronomy Observatory

NEWS GALLERY TELESCOPES + TECH ▾ VISIT US ▾ LEARN ▾ EXPLORE ▾

GIVE

Search …

# ALMA Shows Massive Young Stars Forming in "Chaotic Mess"

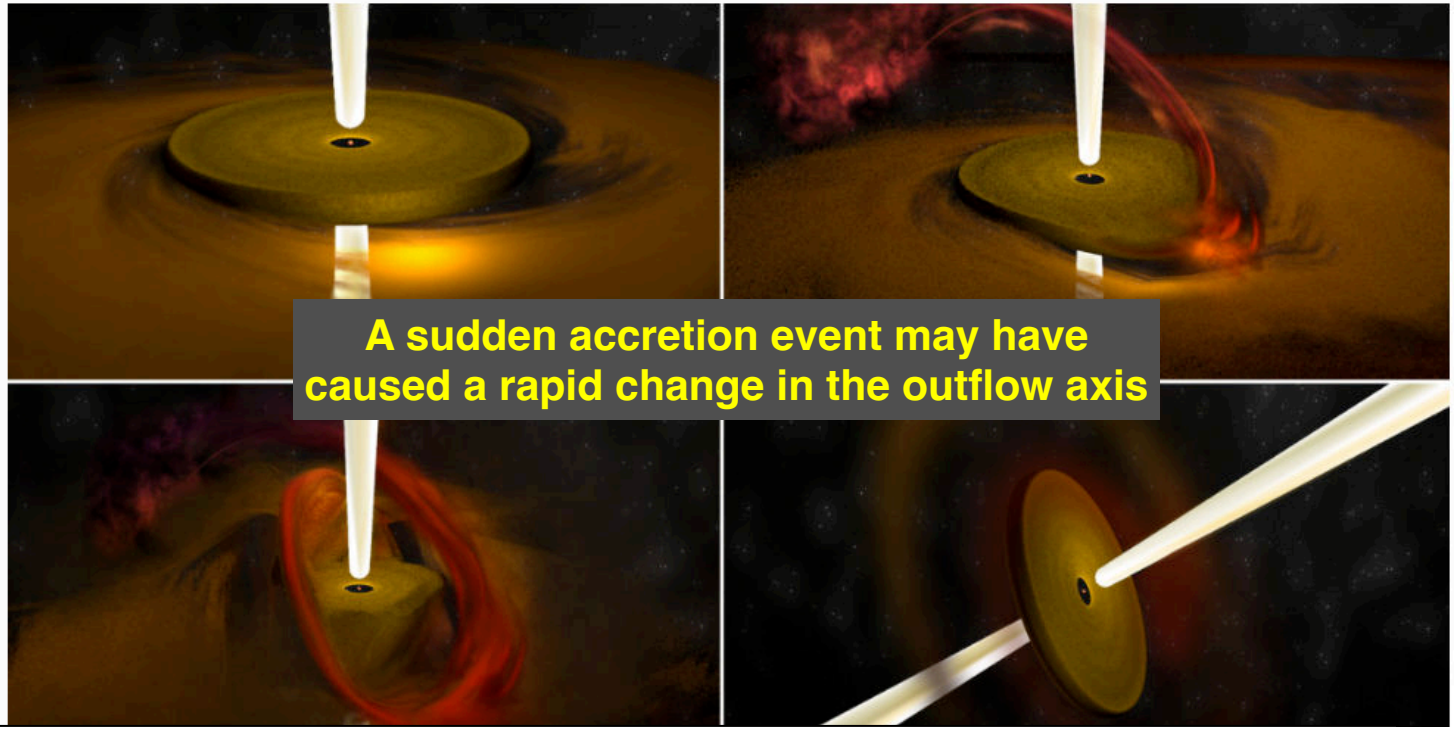


NRAO Press Release https://public.nrao.edu/news/massive-young-stars-forming/. Goddi+ 2020

# Conclusions

I. The feedback from young O stars does not halt SF

II. The stars exciting HC-HII regions show no evidence of ongoing accretion.

III. Accretion in proto-O-stars:

A. is multi-directional via narrow channels or filaments

B. does not involve disks larger than ~100-300 AU

C. is episodic (fast collimated outflows change orientation with distance and/or over time)

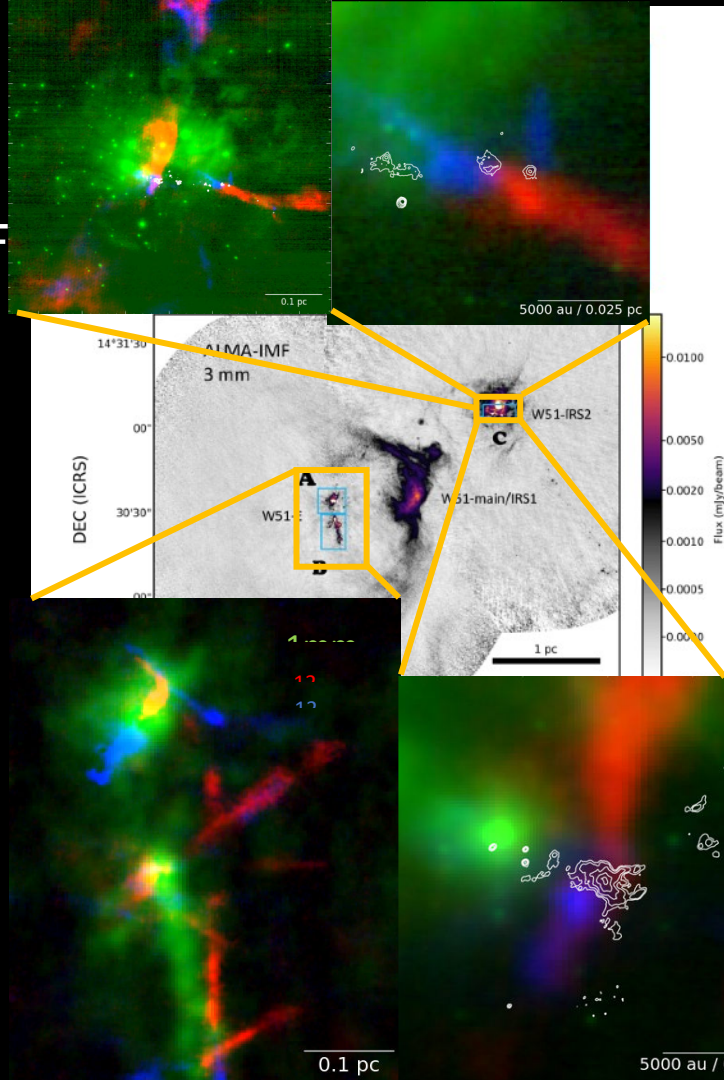

# THANK YOU!!!